Title
Clothing as a transport vector for airborne particles: Chamber study.

Journal
Indoor air, 28(3)

ISSN
0905-6947

Authors
Licina, D
Nazaroff, WW

Publication Date
2018-05-01

DOI
10.1111/ina.12452

Clothing as a transport vector for airborne particles: Chamber study

Journal:	*Indoor Air*
Manuscript ID	Draft
Manuscript Type:	Original Article
Date Submitted by the Author:	n/a
Complete List of Authors:	Licina, Dusan; University of California Berkeley, Civil and Environmental Engineering Nazaroff, William; University of California, Civil & Environmental Engineering
Keywords:	Bioaerosol, Exposure, Hospital-acquired infection, Particulate matter, Personal cloud, Resuspension

Clothing as a transport vector for airborne particles: Chamber study

Dusan Licina*, William W Nazaroff

Department of Civil and Environmental Engineering, University of California, Berkeley, California 94720, United States of America

*Corresponding email: licinadusan@yahoo.com

Abstract

Strong evidence suggests that clothing serves as a reservoir of chemical pollutants and particles, including bioaerosols, which may have health significance. However, little is known about the role that clothing may play as a transport vector for inhaled airborne particles. Here we contribute toward bridging the knowledge gap by conducting experiments to investigate clothing release fraction (CRF), determined as the size-dependent ratio of released to deposited particulate matter in the diameter range 0.5-10 μm. In a fully controlled chamber with low background particle levels, we deployed a programmable robot to reproducibly quantify the size-dependent CRF as a function of motion type and intensity, dust loadings and activity duration. On average, 0.3-3% of deposited particles were subsequently released with fabric motion, confirming that clothing can act as a vehicle for transporting airborne particles. The CRF increased with the vigor of movement and with dust loading. Rubbing and shaking the fabric was more effective than fabric stretching in resuspending particles. We also found that most of the release happened quickly after the onset of the resuspension activity. Particle size substantially influenced the CRF, with larger particles exhibiting higher values.

Practical Implications

The uptake and subsequent release of particles from clothing can influence inhalation exposure of the wearer and, potentially, serve as a means of transferring harmful airborne particles from one location to another. Efforts to quantify the role of clothing as a transport vector for airborne particles is potentially valuable for understanding how bioaerosols are transmitted and potentially controlled.

Keywords

Bioaerosol, Exposure, Hospital-acquired infection, Particulate matter, Personal cloud, Resuspension.

Introduction

Exposure to particulate matter is correlated with adverse health outcomes including infectious disease, asthma, and allergy.[1,2] Hospital patients are particularly vulnerable; patients are vulnerable owing to their health status and nosocomial infections represent a major source of morbidity and mortality worldwide.[3] It is well established that human occupancy and associated activities materially influence the total and biological aerosol burden indoors.[4-10] One potentially overlooked exposure pathway mediated by humans, for which no exhaustive evidence is available, is exposure to aerosols formerly deposited on clothing and subsequently released to air. Characterizing the role of clothing as collector and subsequent emitter of airborne particles is fundamentally important as released particles could become a source of inhalation exposure not only for the wearer but can also to others who share the indoor space.

Sufficient evidence supports the plausibility that clothing acts as a transport vector, moving particulate matter from one environment to another, and thereby causing altered exposures to specific particle-borne agents. McDonagh and Byrne[11] demonstrated that a substantial fraction of particles formerly deposited onto a clothing fabric are subsequently dispersed into the air by means of physical movement. Other studies reported that clothing may play a role in collecting and transferring microbial species into the air, such as *Staphylococcus* *aureus*,[12] fungal spores[13,14] and allergenic pollen.[15-17] A growing concern about clothing as a reservoir for the transmission of microorganisms and pathogens arises in hospitals, owing to the potential involvement in nosocomial infections.[18-20] Dispersal of airborne bacteria in hospitals from contaminated healthcare apparel and textiles has been detected in operating theatres[21,22] and textile storage rooms.[23] Homaira et al.[24] found that respiratory syncytial virus, which is the major cause of respiratory infections among premature infants, can be detected on clothes worn by caregivers and visitors; they suggested that "personnel clothing … may have a role in transmission" in neonatal intensive care units. Although these studies support the plausibility that clothing can act as a vector for aerosol exposure, evidence remains limited that would quantify the significance of this process with regard to particle size, dynamic behaviour, and fate.

Additional evidence demonstrates that clothing surfaces acquire biological material from the wearer's skin and from the surrounding environment.[25,26] For example, it has been estimated that 5 mg of skin flakes is transferred to clothing every hour.[25] By means of DNA-based approaches, studies have shown that clothing surface is home to a diverse population of microorganisms, including bacteria,[27,28] viruses[24] and fungi.[26,29] These microorganisms are potentially dispersed from clothing into air in two ways, both as a result of physical activity of the wearer: i) directly, by releasing previously deposited material; and ii) indirectly, via frictional interactions between clothing fibres, the wearer's skin and other contact surfaces.[21,30,31] While there is no clearly established relationship between clothing-released particles with bioaerosols, recent studies suggest that human-associated particle emissions span the dominant size range of indoor airborne bacteria, and that a fraction of total particle emissions from clothing is linked to bioaerosols.[7,31-34]

For understanding the role of clothing as a vehicle for the transfer of airborne particles, including bioaerosols, it is necessary to study this process quantitatively and mechanistically. Duguid and Wallace[35] were among the first to experimentally investigate the liberation of bacteria-carrying dust particles from the skin and clothing as a result of various bodily movements. They found that movement intensity could generate a 10× increase in the emission rate of dust-borne bacteria. Recent measurements conducted with a high temporal and particle-size resolution showed that, relative to sitting activities, emissions of supermicron (>1 μm) particles increase by 2-5× when occupants engage in more vigorous movements, including walking on a dust-free surface; a possible contributor to these observations is increased frictional interactions between clothing fibres with increased movement vigor.[31,36,37] Folding and putting on and taking off a freshly laundered cotton shirt was found to temporarily increase the particle mass concentration in the breathing zone by >30 μg/m^3.[37] While these studies have added important new knowledge about quantitative and mechanistic aspects of particle release from clothing that could contribute to airborne exposures, little effort was devoted in these works to considering the primary origins of the emitted particles.

To quantify the role of clothing as a potential transport vector for airborne particles, we undertook a set of experiments as reported here. We quantified the release process in terms of a "clothing-release fraction" (CRF), which is the ratio of released to deposited particulate matter resulting from a defined activity following a controlled particle deposition process. The studies were conducted in a chamber that allowed for reproducible contamination of a clothing fabric with particulate matter and subsequent release into the air by means of fabric manipulation utilizing a programmable robot. The objective of the study was to assess the relative importance of the fabric motion type and intensity, dust loadings and activity duration, in relation to the size-resolved CRF. The collection of real-time, size-resolved data allowed us to explore processes associated with the dynamic behavior of particles during deposition and resuspension. The results of this study add knowledge and understanding of the role of clothing in contributing to primary and secondary exposure routes and could ultimately help strengthen particulate-matter exposure and risk assessments. The knowledge gained could also prove worthwhile for characterizing interventions to mitigate the transfer of coarse mode airborne particles, including bioaerosols, from clothing to the respiratory tract.

Methods

Experimental chamber

To simulate environmental uptake of particles onto clothing followed by release resulting from fabric disturbance, we utilized a laboratory-scale, well-controlled chamber (Figure 1). The system was designed to have the essential virtue of allowing effective control of particle deposition and quantification of subsequent release. The chamber has a floor area of 0.58 m^2 (dimensions 76 × 76 cm) and a height of 0.90 m, yielding an interior volume of 0.52 m^3. The aluminum surfaces of the chamber were electrically grounded to reduce electrostatic charge and thereby minimize deposition of particles onto the chamber walls. The chamber was outfitted with a system that supplied air at a constant flow rate of 0.25 m^3/h, corresponding to an air-exchange rate of 0.48 h^{-1}. The empirically derived air-exchange rate, measured by means of carbon dioxide (CO_2) decay,[38] confirmed that the ventilation rate was stable at 0.48 ± 0.01 per hour ($n = 30$ replicates). To prevent intrusion of external sources of particulate matter into the chamber, the supply air was delivered through a high efficiency particulate arrestance (HEPA) filter. To avoid contamination from exogenous PM sources owing to uncontrolled infiltration, the chamber was slightly pressurized. Four mixing fans were mounted on the inner chamber walls to ensure uniform particle deposition onto the fabric and to promote well-mixed conditions during the resuspension event. We measured the average airspeed in the core of the chamber on a 2 × 3 grid by means of a thermal anemometer probe (TSI, Air Velocity Meter Model 9545). The average airspeed was 0.28 ± 0.02 m/s (n = 3), which is comparable to the maximum velocities recorded in the thermal plume enveloping the human body.[39,40] Reported airspeeds for ventilated indoor spaces are similar: 5-20 cm/s in one study[41] and 5-40 cm/s in another.[42] During all experiments, the relative humidity and dry-bulb temperature remained fairly stable (Model U12-012, HOBOware Pro, Onset Computer Co., Bourne, MA, USA): measured values were 35 ± 7% and 24 ± 1.5 ˚C, respectively.

Controlled deposition onto fabric

To prepare the test materials, a newly purchased unsewn black fabric was cut into ten rectangles with dimensions 40.5 × 30 cm (0.122 m^2). The fabrics were sewn along the edges by machine to prevent separation of clothing fibers during multiple treatments. The fabric, made of 65% polyester blended with 35% cotton fibers, was selected to match the material of hospital scrubs typically worn by nurses and other healthcare workers.

Fabric conditions were kept constant throughout the experiments. Prior to controlled contamination by particle deposition, each fabric piece was laundered in cold water with detergent, machine tumble-dried, and sealed in a clean, airtight container. Our data indicate that repeated laundering and drying (up to 6 cycles per fabric piece) did not significantly affect particle resuspension. This study was not designed to probe the effect of different fabric materials, which have been shown in other studies to influence particle resuspension.[11,36]

The clean fabric, affixed to a dust-free solid surface, was placed horizontally at the bottom of the chamber (Figure 1). For each test, a controlled particle loading onto the fabric was performed by means of dispersing a known and reproducible quantity of dust. We used the polydisperse Arizona Test Dust (ISO 12103-1, A1 Ultrafine) in the size range 0.35-20 µm (Powder Technology Inc., Burnsville, MN, USA). According to manufacturer-specified values, 96% of the volume size distribution is associated with particles smaller than 11 µm in diameter. The supplier-reported number and volume size distribution have means at 0.96 µm and 4.78 µm, respectively. This size range of particles spans bacterial and fungal bioaerosol sizes, and also includes particle sizes that would be commonly associated with allergens, pet dander, and mold spores.[43-46] To create a uniform suspension, a specific amount of dust, measured with an analytical balance (Model 1712 Mp8, Sartorius AG, Göttingen, Germany), was loaded into a small discharge tube. The discharge tube with loaded dust was positioned at a chamber side wall and the particles were aerosolized with a 2-s burst of pressurized air supplied at 32 psi. The discharged particles travelled vertically upwards into the well-mixed deposition chamber and then were allowed to settle onto the fabric by means of gravity. To ensure settling of all particle sizes in the dust, the fabric remained in the chamber for 2.5 h after the discharge event. The fans were operated only during the initial 3 min after the dust injection to promote initial mixing and also to limit depositional particle losses on vertical surfaces of the chamber. To confirm that the mixing fans provided uniform particle deposition on the fabric surface, we also collected the dust on nine 47-mm PTFE filters (pore size 0.45 µm, Sartorius AG, Göttingen, Germany) placed on the chamber floor, adjacent to the fabric. Gravimetric analysis by means of a filter microbalance (Model SE2-F, Sartorius AG, Göttingen, Germany) confirmed that the deposited dust loads from three test runs were spatially uniform and also consistent from one run to another, to within ±15%.

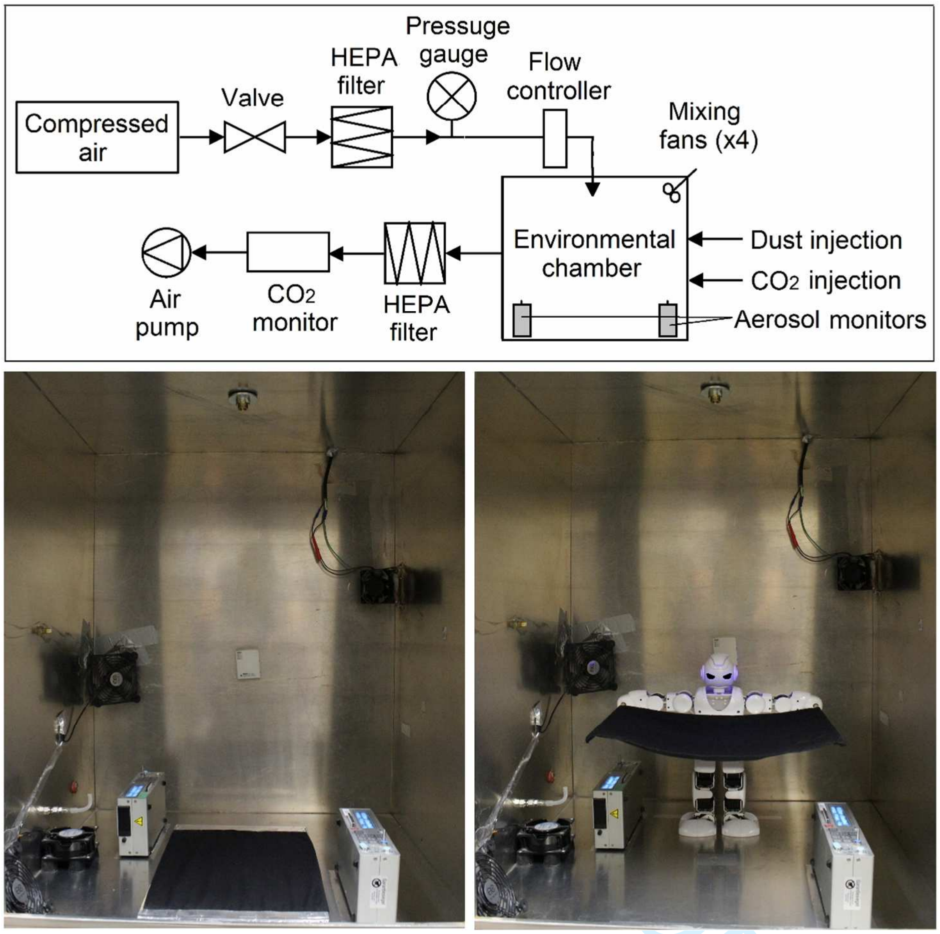

Fig. 1 Schematic of the laboratory-scale chamber configuration (top); photograph of the chamber during deposition event with a fabric on the chamber floor (bottom left); and resuspension event with the robot manipulating the fabric (bottom right). The robot position is for illustration purposes only – during the actual experiments the robot faced the opposite direction (rotated 180˚) with the fabric positioned in the center of the chamber.

Particle resuspension from fabric disturbance

To detect the release of previously deposited particles, fabric disturbance experiments were conducted in the same chamber in which the controlled deposition took place. The chamber was thoroughly cleaned with water and dried between tests to minimize any influence of dust residue on surfaces. To ensure a high level of experimental reproducibility, we used a programmable robot to manipulate the fabrics. The robot (Model Alpha 1S, UBTech Robotics Co.) has 16 independently controllable joints that were programmed to manipulate a fabric in the chamber so as to yield surface vibrations and accelerations designed to be similar to those experienced by hospital scrubs worn by a healthcare worker. To establish appropriate test conditions, we undertook the following preparatory steps: (i) interviewed a healthcare professional to obtain information about typical practices and activities performed in a neonatal intensive care unit (NICU); (ii) deployed five automated vibrational accelerometers (Model: ADXL335) on a hospital scrub to sense and record three-axis acceleration data; and (iii) recruited a volunteer to wear the hospital scrub with attached accelerometers and to mimic healthcare workers' practices in a NICU. A volunteer wearing the hospital scrub performed three types of scripted activities common to nurses' movements in rooms occupied with premature infants: sitting while handling an infant, standing while handling an infant, and walking at a constant pace (100 steps/min). The recorded accelerometer data were used to guide the intensity of motion applied by the robot to the fabric in the test chamber. Information about accelerometer positioning, sensor reading and a data comparison between the surface vibrations produced by the volunteer and the robot are summarized in Figure S1 in the supporting information. A detailed description of each activity is presented in Table S1.

In the resuspension experiment, a particle-laden fabric was attached to the robot using a procedure that ensured minimal fabric disturbance and negligible particle loss. The contaminated fabric was fixed to a solid surface and transferred to a pair of custom-made fabric holders that were attached to the robot (Figure S2). The robot was then carefully placed in the designated area of chamber. Prior to the commencement of the resuspension event, we used ventilation to establish low background particle levels in the chamber. The robot was operated remotely for a prescribed period, after which the chamber was monitored without disturbance for an additional 20 min to measure the concentration decay of particles released from the fabric.

Experimental design and sampling

Experiments (Table 1) were designed to investigate the influence of the type and vigor of fabric manipulation, the duration of activity and the fabric contamination level, on the size-resolved clothing release fraction (CRF). In all, we conducted nine different deposition and resuspension experiments between March and April 2017, and each experiment was replicated at least three times. The experimental runs were executed in a random order to minimize any risk of bias associated with uncontrolled system changes over time.

One basic type of a fabric movement produced by the robot was stretching. We investigated four intensities of this basic fabric movement: low, medium, high and vigorous. The low, medium and high intensity of fabric movement were designed to replicate aerodynamic and mechanical removal forces experienced when a healthcare worker wears hospital scrubs. In particular, fabric stretching with a low intensity mimicked sedentary and standing worker's activities performed with a premature infant (Table S1). High intensity stretching of a fabric produced vibrational forces similar to those experienced by the fabric of a walking healthcare worker (Figure S1). We also probed two other types of common fabric motion: shaking and rubbing. For the purpose of mutual comparison, these movement types had a consistent level of surface vibrations corresponding to vigorous movements beyond those recorded from the volunteer's simulated activities (Figure S1). The video links (Video S1 – Video S6) for each fabric movement type and intensity are presented in supplementary information.

We examined the influence of the two particle loading levels on the CRF — 4 and 16 mg/m^2. The clothing dust loading is substantially lower than those found on hard flooring and carpets (0.1-100 g/m^2)[47] and on mattresses (0.1-1.0 g/m^2).[48,49] To our knowledge, this study is the first to report estimates for the clothing surface dust loading. To determine an appropriate level of dust loading, we undertook the following steps: (i) recruited a volunteer and attached a clean fabric to his chest, (ii) asked the volunteer to perform regular daily activities for 12 hours in an indoor environment; and (iii) attached the worn fabric to the robot and performed the fabric disturbance experiment in the chamber. The mass of particles released from the fabric was used as an input parameter to determine an appropriate dust-loading amount. We found that manipulating a fabric with a controlled surface dust loading of 4 mg/m^2 dislodged particle mass at a level similar to that released from the fabric worn indoors for 12 h. (See Figure S3.) The dust loading of 16 mg/m^2 is designed to represent more contaminated clothing conditions, for example as a consequence of environmental uptake of particles in polluted areas or because of being worn over multiday periods.

We also undertook experiments to investigate the effect of activity duration on the CRF. For the baseline experiments, a one-minute period of fabric disturbance was consistently used. We investigated two other durations of fabric disturbance activity: 20 sec and 3 min. In addition to the basic factors examined (Table 1), we also probed the influence of the contact time between particle deposition and subsequent fabric disturbance. Evidence suggests that the presence of particles on surfaces causes deformation over time that may gradually enhance the adhesive forces.[50] Consequently, we suspected that longer periods of attachment prior to disturbance could lead to lower transfer factors. In these experiments, particle attachment duration on the fabric was manipulated by controlling the time between particle deposition and subsequent fabric disturbance. We assessed contact time scales of 0.5 h and 48 h during which the contaminated fabric loaded was stored in a clean and airtight container. Results indicate that the variable time of contact caused only small differences (less than 10%) in the resuspended particle mass from the fabric. (Data not shown.)

To measure particle concentrations, both during the deposition period and during the subsequent release experiment, we employed two Grimm aerosol spectrometers (model 11-A, GRIMM Aerosol Technik GmbH, Ainring, Germany) that provide time-and size-resolved data (31 size channels from 0.25 to 32 µm) for aerosol particles. The particle size range of interest spanned the optical diameter range from 0.5 to 10 µm, with reporting in 17 size channels. The two monitors were positioned at the bottom of the chamber (Figure 1). The recordings of two monitors agreed to within 3% during deposition and to within 5% during resuspension experiments, confirming that the conditions were well mixed in the chamber. Simultaneously, CO_2 levels were recorded to allow for determination of air-exchange rate by means of tracer-gas decay. For this purpose, we employed a real-time gas analyzer (LI-COR Biosciences, Lincoln, NE, USA). For all time-resolved measurements, we adopted 1-min sampling intervals to accurately capture the dynamically changing conditions.

Data interpretation

For the purpose of converting particle number concentration into particle mass, we assumed that particles are spherical and that the mass-weighted size distribution, $dM/d(\log d_p)$, is constant within each particle size channel. The manufacturer-specified density of the dust particles, 2.5 g/cm^3, is assumed to apply for each size section.

Particles injected into the chamber are lost from air by combination of ventilation (though instrument sampling) and deposition onto surfaces. Particle deposition was quantified based on the approximation that all particles are lost by settling onto upward facing surfaces only. The size-specific time-averaged mass of deposited particles on the fabric can be expressed through the following equation:

$$M_{i,dep} = \overline{C_i(T)} \times T \times k_i \times V \times \frac{A_f}{A} \qquad (1)$$

In equation (1), $\overline{C_i(T)}$ is the size-specific particle mass concentration (µg/m^3) averaged across period T, which starts at zero (particle injection) and finishes when particle concentration decays to the background value (after 2.5 h); k_i is the size-dependent particle deposition loss-rate coefficient (h^{-1}); V is the volume of the chamber (m^3); and A_f/A is the ratio of fabric area to chamber floor area. The deposition rate terms, k_i, were derived for each run based on the size-dependent particle number concentrations measured during the decay period. We determined the k_i value by subtracting the air-exchange rate from the absolute value of the slope of the natural logarithm of C_i versus decay time. (Results are reported in Figure S4.)

The recorded data during fabric disturbance events were analyzed using a material-balance approach to extract quantitative information about particle source strengths and decay rates.[51,52] The resuspended particles are lost from chamber air by a combination of deposition and ventilation:

$$M_{i,res} = \overline{C_i(T)} \times T \times V \times (k_i + a) \tag{2}$$

Here, the period T starts at the beginning of the resuspension activity and continues until the particle concentration decays to the background (after 20 min); a is the air-exchange rate (1/h). Repeated runs (n = 30) indicate that empirically derived deposition loss-rate coefficients (k_i) were stable throughout deposition and resuspension experiments, given that the properties of particles and chamber environment did not change, which is evident from the low standard deviations displayed in Figure S4. Therefore, we adopted a single set of mean values of k_i (one for each size section), which was applied to all experimental runs. The clothing release fraction (CRF) is evaluated for each particle size section (17 size sections in the range 0.5-10 µm) as the ratio of the particle mass released normalized by the mass of particles previously deposited on the fabric. Since the effect of fabric manipulation did not have significant effect on resuspending particles smaller than 1 µm, the CRF results are presented only for the size range 1-10 µm.

Quality assurance

Data collected with the two calibrated aerosol spectrometers agreed well across the particle size spectrum of interest; hence, no correction factors were applied. The performance of CO_2 monitor was confirmed by exposing the instrument to calibration gases at 0 and 1000 ppm.

For each resuspension event, we performed “blank” experiments with freshly laundered fabric to permit quantitative differentiation from particles that were artificially seeded onto the fabric. The freshly laundered fabric samples were subjected to the same disturbance procedures established during the controlled experiments. The released particle mass was consistently small in these background experiments, always <5% of the total mass released from the contaminated fabric. The background release values were subtracted from the measured results during release experiments to minimize measurement inaccuracy.

Results and Discussion

Figure 2 displays time series of size-dependent airborne particle number concentrations measured during controlled deposition and resuspension periods for one representative experiment (ID = 3; see Table 1). Upon initial dust injection, there is a sharp spike in the particle number concentration after which concentrations decline as particles settle. The larger particles, with higher gravitational settling velocities, quickly decreased to background levels. For smaller particles (0.5-1 µm) that remain airborne longer, we found that 2.5 h is a sufficient period for deposition to approach completion so as to restore the background concentrations. Prior to commencement of the resuspension event, the background particle levels were low, confirming that aerodynamic forces from the mixing fans do not overcome the adhesive forces that hold particles to the fabric surface.

The commencement of the resuspension event coincides with the sudden increase of airborne particle concentrations across the size spectrum of interest (0.5-10 µm). We observed that the number of particles in the size range 0.5-1 µm increased to a moderate extent, whereas the concentration of particles larger than 1 µm (1-10 µm) increased by one or more orders of magnitude relative to the background. The observation that fabric disturbance primarily resuspended supermicron particles (>1 µm) is consistent with prior published evidence, showing, for example, that occupancy-associated emissions through particle resuspension from clothing contributes more to coarse particle load as compared to fine particles.[31,37] We also found that, after resuspension, it took approximately 20 min for the concentration of the smallest resuspended particles (0.5-1 µm) to decay to the background value.

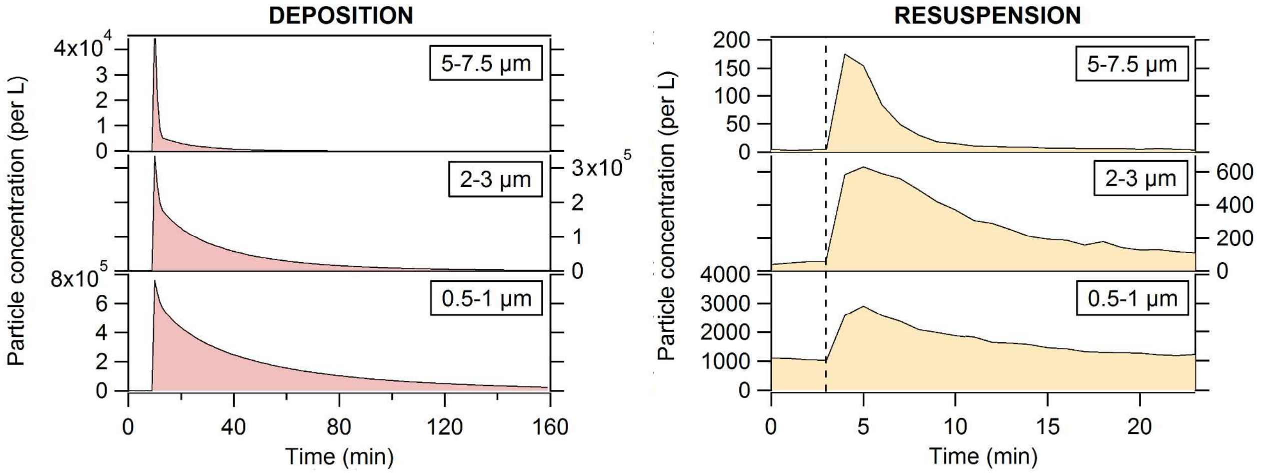

Fig. 2 Example of time series representations (1-min resolution) of the size-segregated particle number concentrations (0.5-1, 2-3, 5-7.5 µm) during a deposition event (left) and a resuspension event (right) for one representative experiment (ID = 3; *n* = 6 replicates). Note that the decay period was continued for 2.5 hours during deposition and for 20 minutes during resuspension. The vertical dashed line indicates the commencement of the resuspension event.

Experimental data for particle number concentrations in each size channel were used to evaluate the size-resolved particle mass during deposition and resuspension events. Figure 3 compares normalized size distributions of average particle number (upper frames) and mass (lower frames) during deposition (left frames) and resuspension events (right frames) for a single representative experiment (ID = 3). Analogous results for other experimental runs are presented in Figure S5. The count-median diameters were approximately 1.2 µm for both deposition and resuspension. Mass median diameters for deposition and resuspension events were shifted to larger particle sizes, 3.8 and 5.0 µm, respectively.

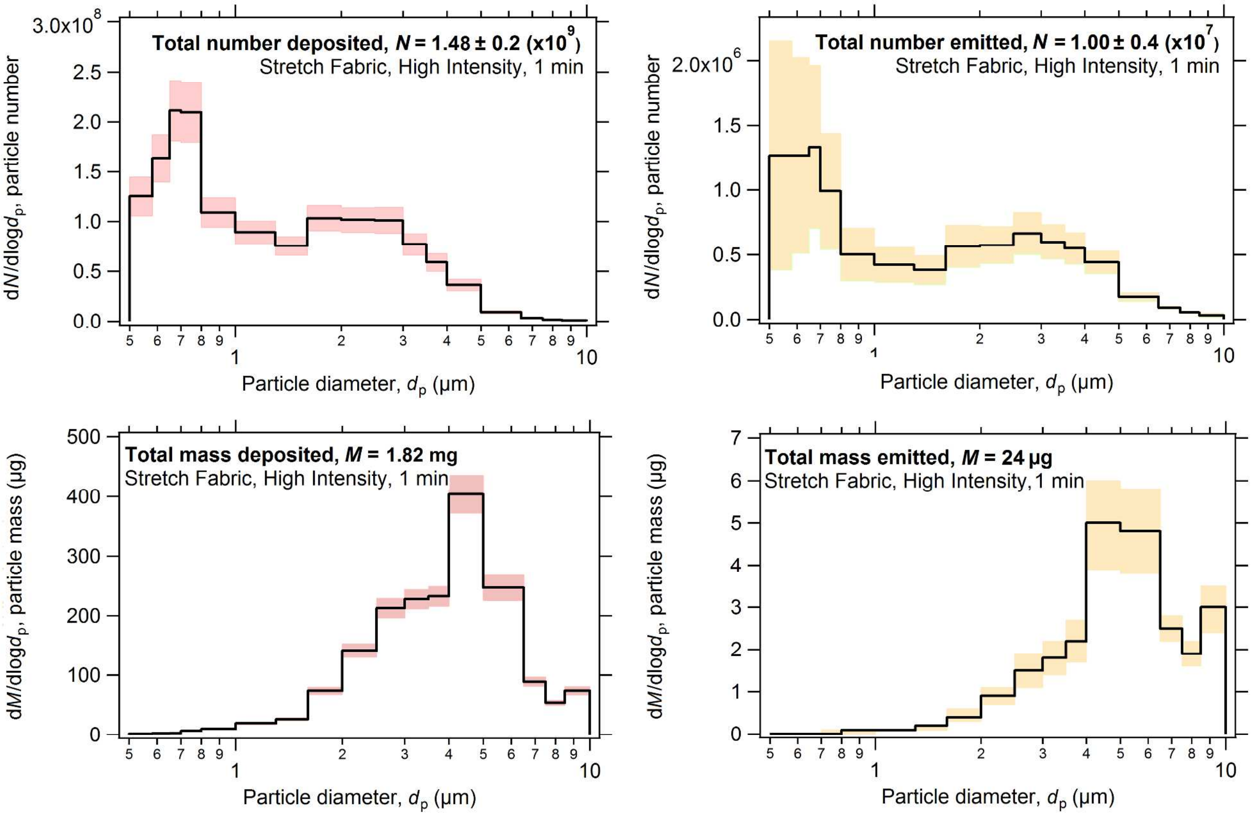

Fig. 3 Size distribution of average particle number (upper frames) and mass (lower frames) during deposition (left frames) and resuspension events (right frames) associated with fabric manipulation. The mean ± standard deviation (illustrated by shaded area) are reported in each frame. These data are for experiment ID = 3, with *n* = 6 replicates.

As seen in Figure 3, there is a difference of approximately two orders of magnitude when comparing the particles deposited to particles resuspended. Removal forces produced by 1-min of motion scaled to simulate regular human movements dislodge a small proportion of deposited particles, while the large majority remain attached to the fabric surface.

We assessed the ratio of particle mass resuspended to particle mass deposited for each of the experimental conditions. Table 1 presents a summary of the clothing resuspension fraction (CRF) for the nine experimental conditions tested. In this table, the CRF is based on the total mass resuspended divided by the total mass deposited. The specific quantitative results are sensitive to the size distribution of the deposited particles, since coarse particles tend to be resuspended more effectively than fine particles. When considering factors such as the type and vigor of motion, the aggregate CRF results displayed in Table 1 span about an order of magnitude range, from 0.3 to 3%.

Table 1 Summary of clothing experiments: mean ± standard deviation of particle mass (0.5-10 μm) during the deposition and resuspension event; and the resultant clothing resuspension fraction (CRF). [a, b]

ID	**Motion**	**Intensity**	**Duration (min)**	**Loading (mg/m^2)**	**Deposited (mg)**	**Resuspended (μg)**	**CRF (%)**
1	Stretch Fabric	Low	1	16	1.7 ± 0.1	5.0 ± 1.2	0.3 ± 0.1
2	Stretch Fabric	Medium	1	16	1.7 ± 0.3	11 ± 2.8	0.7 ± 0.1
3	Stretch Fabric	High	1	16	1.8 ± 0.3	24 ± 4.5	1.3 ± 0.2
4	Stretch Fabric	Vigorous	1	16	1.9 ± 0.1	36 ± 6.7	1.9 ± 0.3
5	Shake Fabric	Vigorous	1	16	1.7 ± 0.2	46 ± 4.8	2.6 ± 0.4
6	Rub Fabric	Vigorous	1	16	1.8 ± 0.1	53 ± 3.5	3.0 ± 0.3
7	Stretch Fabric	High	1	4	0.5 ± 0.05	2.7 ± 0.9	0.6 ± 0.2
8	Stretch Fabric	High	0.33	16	1.9 ± 0.3	19 ± 5.4	1.0 ± 0.1
9	Stretch Fabric	High	3	16	1.5 ± 0.2	26 ± 6.2	1.8 ± 0.3

[a] For each experiment there were *n* = 3 replicates, except for the reference scenario, ID = 3, for which 6 replicates were conducted.

[b] Two supplementary experiments were conducted. In the first, resuspension was tested 48 h after the deposition event to probe the effect of the particle residence time on clothing fibers on the CRF. The effect was found to be insignificant. The second test included fabric manipulation that was previously worn by human subject for 12 hours to examine particle loading quantity. Those results are shown in Figure S2.

Clothing resuspension fraction: Influence of activity intensity and type

Figure 4 presents a summary of size-resolved CRFs as a result of fabric disturbance by means of stretching with different intensities. For this one type of motion, the aggregate resuspended fractions (on a mass-weighted basis) spanned about a factor of 6, from 0.3% to 1.9%, systematically increasing with the intensity of motion. This range of values is similar to the upper end of resuspension fractions reported for flooring surfaces, 10^{-7} to 10^{-2}.[47,53-55]

Figure 4 also demonstrates a systematic increase in the resuspension fraction with increasing particle size. Over the range of particle sizes displayed, spanning 1 to 10 µm optical diameter, there is about an order of magnitude difference between the fractions resuspended for the largest compared with the smallest particles. This general pattern — an upward trend in resuspended fraction as a function of particle size — was exhibited for all cases studied. Qualitatively, this result is expected. Dislodging forces owing to acceleration would scale with particle inertia (i.e., in proportion to particle diameter cubed). Adhesion forces would increase with particle size more gradually. Consequently, the ratio of dislodging forces to adhesion forces is expected to increase with increasing particle size. Such behaviour is consistent with theory[56] and with prior experimental observations.[57,58]

Interestingly, doubling the vibrational forces from low to medium intensity yielded twice the value of the CRF; however, increasing the fabric vibration by 2× from high to vigorous intensity was associated with only a 40% higher release fraction. Hence, the relationship between the vibrational forces and the CRF does not appear to be linear. One study reported that vigorous shake off of clothes, at surface vibrations well beyond those used in our study, can reduce the amount of pollen adhering to the surface by less than half.[16]

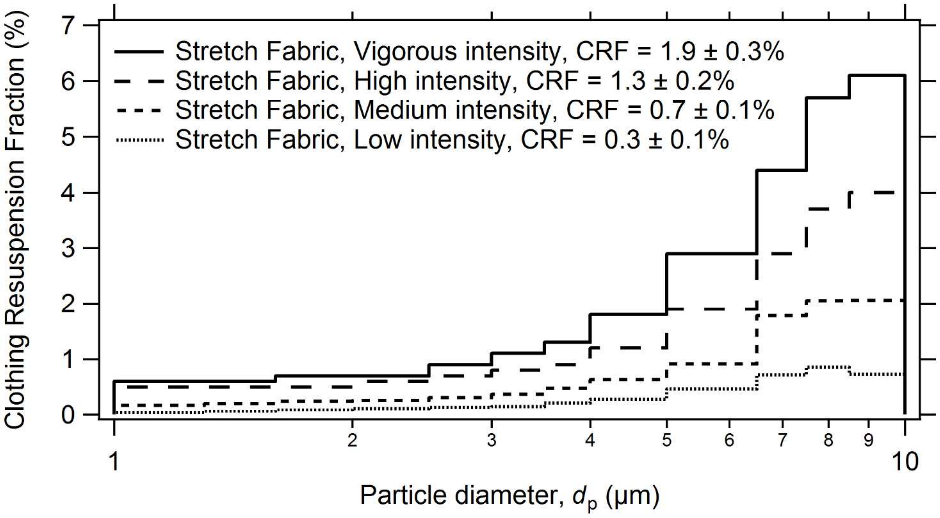

Fig. 4 Size distribution of average clothing resuspension fraction as a consequence of manipulating contaminated fabric with different activity intensities.

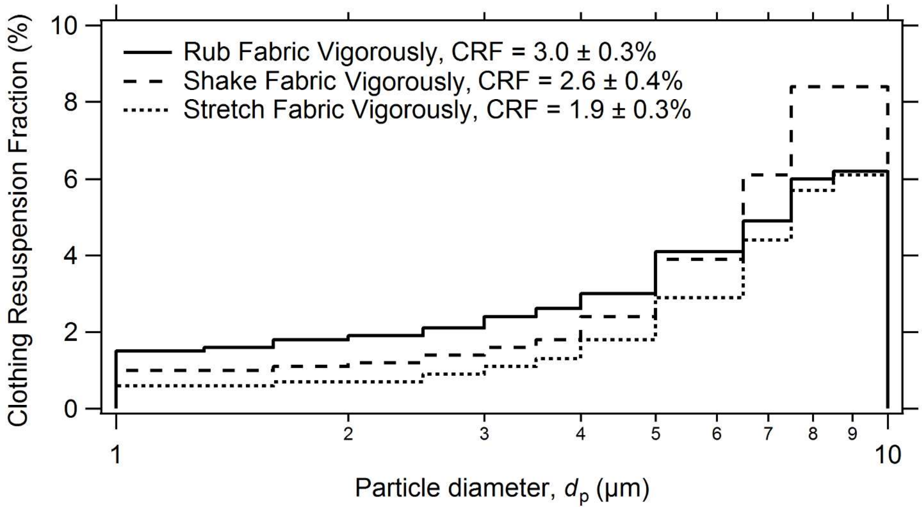

Fig. 5 Size distribution of clothing resuspension fractions as a consequence of manipulating particle-loaded fabric using different types of motions. Note that the resultant clothing surface vibrations during these three activities were comparable to one another.

Figure 5 displays the size distribution of the CRF for vigorous motion, comparing three common types of fabric movements. Overall, rubbing the fabric was associated with the highest CRF, releasing 3% of the total deposited particles in the size range 1-10 μm. Rubbing the fabric dislodged somewhat more particles compared to shaking and stretching motions. Likely, the higher release from rubbing reflects additional removal forces caused by mechanical abrasion as a consequence of clothing fibres rubbing against each other and (potentially) contacting deposited particles. The CRF increased with particle size across all activities, but not identically. In particular, the shaking motion resuspended the highest proportion of large particles, with the CRF peaking at ~8% in the size range 7.5-10 µm.

Clothing resuspension fraction: Influence of particle loading level and activity duration

Figure 6 shows the size-resolved CRF as a function of two dust loading levels: 4 and 16 mg/m^2. We were surprised to find that surface dust loading significantly affected the resuspension fraction. At a surface dust loading of 4 mg/m^2, the CRF was 0.6%, approximately 2× lower than with a loading of 16 mg/m^3. These findings are consistent with previously reported observation of increased fraction of resuspended particles at higher surface loadings on hardwood and vinyl flooring.[55] Other findings indicate that resuspended fraction can either decrease, increase or remain unchanged at higher surface dust loadings, contingent on the surface material and porosity, relative humidity, particle size and penetration, and deposit type.[11,49,55,59] The scale of dust loadings used in our study are most likely to yield a less-than monolayer deposit. Consequently, contact for deposited particles would be primarily with fabric fibers, rather than with other deposited particles. The higher release fraction with a higher loading suggests the possibility that sites vary with regard to attachment force in such a way that the more strongly adherent locations are preferentially filled; if so, then as the loading increases the average attachment force would diminish.

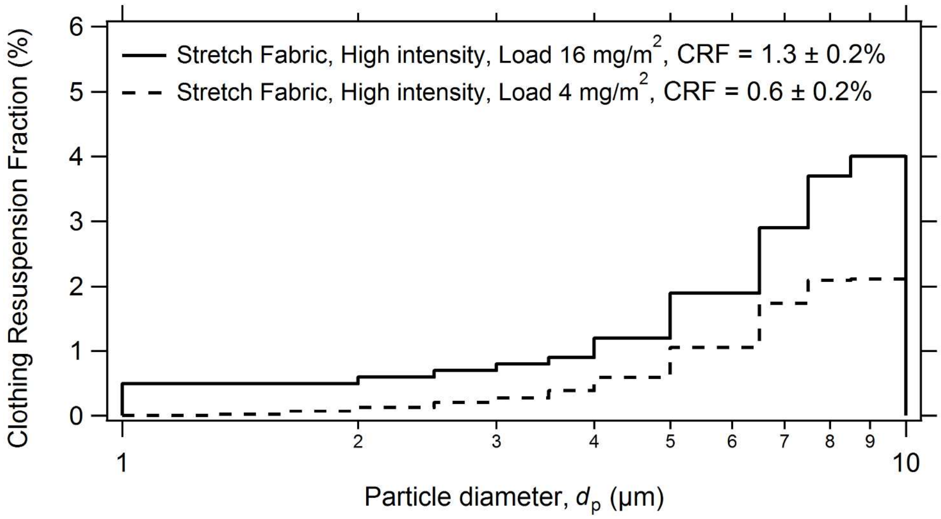

Fig. 6 Size distribution of average clothing resuspension fraction as a consequence of manipulating fabric by means of high-intensity stretching. The fabrics were treated with two different dust loading amounts: 4 and 16 mg/m^2.

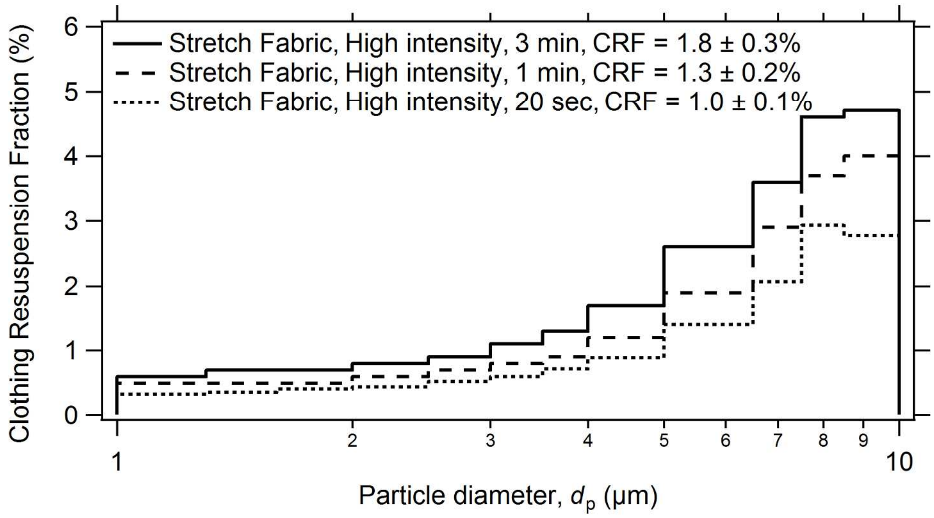

Fig. 7 Size distribution of average clothing resuspension fraction as a consequence of continuous manipulation of contaminated fabric for different durations.

Figure 7 shows that the CRF is not linearly related to activity duration. In particular, for the conditions tested, approximately half of dislodged particles were released early, within the initial 20 seconds of resuspension movement. With time, the CRF continued to increase, but at a progressively smaller rate. Overall, 3× longer fabric agitation led to only 1.3× higher particle transfer rate, while extending the activity by 9× caused a 1.8× higher CRF than the shortest agitation period.

Study strengths and limitations

The current experiments were conducted in a small-scale chamber which is suitable for quantitative evaluation of particle release under controlled manipulation conditions. This study included an investigation of the effects of several independent variables: particle size, motion type, motion vigor, and motion duration. However, the investigation is restricted to one type of particle, one fabric material, one type of particle deposition process, and controlled resuspension motions. This type of research would benefit from examining the influence of different types of particle sources (size distribution, shape, composition and concentrations) that are commonly encountered in both outdoor and indoor air. The reported CRF values are also conditional because we did not study the influence of relative humidity and fabric moisture content, which are known to influence resuspension.[60-62] Notwithstanding the apparent limitations, the reproducibility of the results presented here, as a consequence of tightly controlled environmental conditions (including use of a programmable robot), allowed for quantitative investigation of some parameters that have not been previously characterized.

Future outlook

The present study builds upon the emerging evidence that clothing can act as a vector for airborne particle transmission. To further advance the state of knowledge on this topic, the evaluated clothing release fractions from these experiments need be compared to those obtained in actual built environments as a means of testing the relevance of the laboratory investigations to inform full-scale release conditions. Although this issue could be addressed in many room types, hospitals provide a study location that is well suited for such investigations because their environments are highly controlled and the occupancy patterns are relatively well defined. There also is a need to quantify the relative contribution of clothing-released particles to indoor exposures, which is ultimately important in relation to how indoor air quality influences human health.

In the context of bioaerosol exposure in health care facilities, humans are recognized sources of airborne fungal and bacterial species.[63,64] Other recognized sources of microbial communities include fixed surfaces of rooms and furnishings,[65,66] wastes[67,68] and various textiles, including beddings and hospital scrubs,[23,69] but the relative contribution of each is unknown.[70] Despite notable progress in infection control, through HEPA filtration of ventilation air, stringent surface cleaning, and strict hand-washing policies, nosocomial infections remain a major concern. The stubborn persistence of hospital-acquired infections substantiates the need for better understanding of alternative sources of bioaerosols and dispersal pathways that may be overlooked by conventional hygiene interventions and other environmental management strategies. It seems worthwhile to consider whether the incidence of nosocomial infections can be suppressed by limiting human-associated bioaerosol transmission through tracking on clothes and subsequent release. It would be of value to conduct studies similar to this one in which the specific focus was on bioaerosol deposition and release. Advances in fluorescence-based real-time monitoring appear promising as a means to design and execute experiments to probe carefully the important dynamic processes that influence bioaerosol dynamic behavior in the perihuman space.

Conclusions

We utilized a well-controlled chamber to investigate the role of clothing as a transport vector for airborne particles that contribute to inhalation exposures. To estimate the size-dependent clothing release fraction (CRF), a programmable robot reproducibly agitated a hospital scrub-like fabric that had been previously loaded with a well-characterized quantity of test dust. Significant release of airborne particles was detected when the particle-laden fabric was agitated (CRF = 0.3-3%, on average), confirming that clothing could serve as mechanism for transferring airborne particles from one location to another. The fraction of deposited particles released increased with particle size, suggesting that coarse-mode bioaerosols could also be effectively transported by means of clothing. Increasing the vigor of fabric motion caused an increase in the CRF, but not linearly. We found that the type of motion influenced resuspension: rubbing and shaking dislodged more particles compared to stretching. Interestingly, the majority of particle release occurred shortly after the onset of the movement. We found that particle transfer can be influenced by the surface dust loading level, with higher CRF observed for a more contaminated fabric.

The present study suggests that environmental uptake of particles onto clothing fabrics and subsequent release may be an important yet overlooked source mechanism contributing to total airborne particle burden in proximity to people. Further efforts to quantify the role of occupant clothing as a transport vector for airborne particle transmission offers the promise of better prediction and control of inhalation exposure in hospital environments and more broadly, to all indoor environments.

Acknowledgements

The research was funded by a grant from the Alfred P. Sloan Foundation. We thank Randy Maddalena for arranging access to the microbalance at the Lawrence Berkeley National Laboratory and Veronika Földváry for her diverse assistance in this project.

References

1. Douwes J, Thorne P, Pearce N, Heederik D. Bioaerosol health effects and exposure assessment: progress and prospects. *Ann Occup Hyg.* 2003;47:187–200.
2. Selgrade MK, Plopper CG, Gilmour MI, Conolly RB, Foos BSP. Assessing the health effects and risks associated with children's inhalation exposures — asthma and allergy. *J Toxicol Environ Health A.* 2008;71:196–207.
3. Cardo D, Dennehy PH, Halverson P, et al. Moving toward elimination of healthcare-associated infections: A call to action. *Infect Cont Hosp Ep*. 2010;31:1101–1105.
4. Fox A, Harley W, Feigley C, Salzberg D, Sebastian A, Larsson L. Increased levels of bacterial markers and CO_2 in occupied school rooms. *J Environ Monitor.* 2003;5:246–252.
5. Chen Q, Hildemann LM. The effects of human activities on exposure to particulate matter and bioaerosols in residential homes. *Environ Sci Technol.* 2009;43:4641–4646.
6. Domanico R, Davis DK, Coleman F, Davis BO. Documenting the NICU design dilemma: comparative patient progress in open-ward and single family room units. *J Perinatol*. 2011;31:281–288.
7. Bhangar S, Huffman JA, Nazaroff WW. Size-resolved fluorescent biological aerosol particle concentrations and occupant emissions in a university classroom. *Indoor Air.* 2014;24:604–617.
8. Bhangar S, Brooks B, Firek B, et al. Pilot study of sources and concentrations of size-resolved airborne particles in a neonatal intensive care unit. *Build Environ.* 2016;106:10–19.
9. Licina D, Bhangar S, Brooks B, et al. Concentrations and sources of airborne particles in a neonatal intensive care unit. *PLoS ONE.* 2016;11:e0154991.
10. He C, Mackay IM, Ramsay K, et al. Particle and bioaerosol characteristics in a paediatric intensive care unit. *Environ Int.* 2017;107:89–99.
11. McDonagh A, Byrne MA. The influence of human physical activity and contaminated clothing type on particle resuspension. *J Environ Radioact.* 2014;127:119–126.
12. Hambraeus A. Transfer of *Staphylococcus aureus* via nurses' uniforms. *J Hyg.* 1973;71:799–814.
13. Pasanen AL, Kalliokoski P, Pasanen P, Salmi T, Tossavainen A. Fungi carried from farmers' work into farm homes. *Am Ind Hyg Assoc J.* 1989;50:631–633.
14. Adams RI, Bhangar S, Pasut W, et al. Chamber bioaerosol study: Outdoor air and human occupants as sources of indoor airborne microbes. *PLoS ONE*. 2015;10:e0128022.
15. Zavada MS, McGraw SM, Miller MA. The role of clothing fabrics as passive pollen collectors in the north-eastern United States. *Grana*. 2007;46:285–291.
16. Takahashi Y, Takano K, Suzuki M, et al. Two routes for pollen entering indoors: ventilation and clothes. *J Investig Allergol Clin Immunol.* 2008;18:382–388.
17. Jantunen J, Saarinen K. Pollen transport by clothes. *Aerobiologia*. 2011;27:339–343.
18. Oliveira AC, Silva MDM, Garbaccio JL. Clothing of health care professional as potential reservoirs of micro-organisms: an integrative review. *Texto Contexto — Enferm.* 2012;21:684–691.
19. Fijan S, Turk SŠ. Hospital textiles, are they a possible vehicle for healthcare-associated infections? *Int J Environ Res Public Health*. 2012;9:3330–3343.
20. Mitchell A, Spencer M, Edmiston Jr C. Role of healthcare apparel and other healthcare textiles in the transmission of pathogens: a review of the literature. *J Hosp Infect.* 2015;90:285–292.

21. Doig CM. The effect of clothing on the dissemination of bacteria in operating theaters. *Br J Surg.* 1972;59:878–881.
22. Whyte W, Vesley D, Hodgson R. Bacterial dispersion in relation to operating room clothing. *J Hyg.* 1976;76:367–378.
23. Handorean A, Robertson CE, Harris JK, et al. Microbial aerosol liberation from soiled textiles isolated during routine residuals handling in a modern health care setting. *Microbiome*. 2015;3:72.
24. Homaira N, Sheils J, Stelzer-Braid S, et al. Respiratory syncytial virus is present in the neonatal intensive care unit. *J Med Virol.* 2016;88:196–201.
25. Noble WC. Dispersal of skin microorganisms. *Br J Dermatol.* 1975;93:477–485.
26. Adams RI, Miletto M, Taylor JW, Bruns TD. The diversity and distribution of fungi on residential surfaces. *PLoS ONE*. 2013;8:e78866.
27. Loh W, Ng VV, Holton J. Bacterial flora on the white coats of medical students. *J Hosp Infect.* 2000;45:65–68.
28. Snyder GM, Thorn KA, Furuno JP, et al. Detection of methicillin-resistant *Staphylococcus aureus* and vancomycin-resistant enterococci on the gowns and gloves of healthcare workers. *Infect Control Hosp Epidemiol.* 2008;29:583–589.
29. Neely AN, Orloff MM. Survival of some medically important fungi on hospital fabrics and plastics. *J Clin Microbiol.* 2001;39:3360–3361.
30. Hall GS, Mackintosh CA, Hoffman PN. The dispersal of bacteria and skin scales from the body after showering and after application of a skin lotion. *J Hyg.* 1986;97:289–298.
31. Bhangar S, Adams RI, Pasut W, et al. Chamber bioaerosol study: human emissions of size-resolved fluorescent biological aerosol particles. *Indoor Air*. 2016;26:193–206.
32. Qian J, Hospodsky D, Yamamoto N, Nazaroff WW, Peccia J. Size-resolved emission rates of airborne bacteria and fungi in an occupied classroom. *Indoor Air*. 2012;22:339–351.
33. Hospodsky D, Yamamoto N, Nazaroff WW, Miller D, Gorthala S, Peccia J. Characterizing airborne fungal and bacterial concentrations and emission rates in six occupied children's classrooms. *Indoor Air.* 2015;25:641–652.
34. Zhou J, Fang W, Cao Q, Chang VWC, Nazaroff WW. Influence of moisturizer and relative humidity on human emissions of fluorescent biological aerosol particles. *Indoor Air*. 2017;27:587–598.
35. Duguid JP, Wallace AT. Air infection with dust liberated from clothing. *Lancet.* 1948;252:845–849.
36. You R, Cui W, Chen C, Zhao B. Measuring the short-term emission rates of particles in the "personal cloud" with different clothes and activity intensities in a sealed chamber. *Aerosol Air Qual Res.* 2013;13:911–921.
37. Licina D, Tian Y, Nazaroff WW. Emission rates and the personal cloud effect associated with particle release from the perihuman environment. *Indoor Air*. 2017;27:791–802.
38. Persily AK. Evaluating building IAQ and ventilation with indoor carbon dioxide. *ASHRAE Trans.* 1997;103:193–204.
39. Craven BA, Settles GS. A computational and experimental investigation of the human thermal plume. *J Fluid Eng.* 2006;128:1251–1258.
40. Licina D, Pantelic J, Melikov A, Sekhar C, Tham KW. Experimental investigation of the human convective boundary layer in a quiescent indoor environment. *Build Environ.* 2014;75:79–91.

41. Hanzawa H, Melikov AK, Fanger PO. Airflow characteristics in the occupied zone of ventilated spaces. *ASHRAE Trans.* 1987;93:524–539.
42. Thorshauge J. Air-velocity fluctuations in the occupied zone of ventilated spaces. *ASHRAE Trans.* 1982;88:753–764.
43. Bernard HR, Speers R, O'Grady FW. Shooter RA. Airborne bacterial contamination: investigation of human sources. *Arch Surg.* 1965;91:530–533.
44. D'Amato G, Spieksma FTM. Aerobiologic and clinical aspects of mould allergy in Europe. *Allergy*. 1995;50:870–877.
45. Hamilton RG. Assessment of indoor allergen exposure. *Curr Allergy Asthma Rep.* 2005;5:394–401.
46. Zahradnik E, Raulf M. Animal allergens and their presence in the environment. *Front Immunol*. 2014;5:76.
47. Qian J, Peccia J, Ferro AR. Walking-induced particle resuspension in indoor environments. *Atmos Environ.* 2014;89:464–481.
48. Gehring U, Bischof W, Borte M, et al. Levels and predictors of endotoxin in mattress dust samples from East and West German homes. *Indoor Air.* 2004;14:284–292.
49. Boor BE, Spilak MP, Corsi RL, Novoselac A. Characterizing particle resuspension from mattresses: chamber study. *Indoor Air.* 2015;25:441–456.
50. Krishnan S, Busnaina AA, Rimai DS, Demejo LP. The adhesion-induced deformation and the removal of submicrometer particles. *J Adhes Sci Technol.* 1994;8:1357–1370.
51. Nazaroff WW. Indoor particle dynamics. *Indoor Air.* 2004;14(Suppl.7):175–183.
52. Ferro AR, Kopperud RJ, Hildemann LM. Source strengths for indoor human activities that resuspend particulate matter. *Environ Sci Technol.* 2004;38:1759–1764.
53. Gomes C, Freihaut J, Bahnfleth W. Resuspension of allergen-containing particles under mechanical and aerodynamic disturbances from human walking. *Atmos Environ.* 2007;41:5257–5270.
54. Qian J, Ferro AR. Resuspension of dust particles in a chamber and associated environmental factors. *Aerosol Sci Technol*. 2008;42:566–578.
55. Tian Y, Sul K, Qian J, Mondal S, Ferro AR. A comparative study of walking-induced dust resuspension using a consistent test mechanism. *Indoor Air.* 2014;24:592–603.
56. Hinds WC. *Aerosol Technology: Properties, Behavior, and Measurement of Airborne Particles.* New York, NY: John Wiley & Sons, Inc.; 1999.
57. Katainen J, Paajanen M, Ahtola E, Pore V, Lahtinen J. Adhesion as an interplay between particle size and surface roughness. *J Colloid Interface Sci.* 2006;304:524–529.
58. Felicetti MA, Piantino F, Coury JR, Aguiar ML. Influence of removal time and particle size on the particle substrate adhesion force. *Braz J Chem Eng.* 2008;25:71–82.
59. Boor BE, Siegel JA, Novoselac A. Wind tunnel study on aerodynamic particle resuspension from monolayer and multilayer deposits on linoleum flooring and galvanized sheet metal. *Aerosol Sci Tech.* 2013;47:848–857.
60. Busnaina AA, Elsawy T. The effect of relative humidity on particle adhesion and removal. *J Adhes.* 2000;74:391–409.
61. Jones R, Pollock HM, Geldart D, Verlinden A. Inter-particle forces in cohesive powders studied by AFM: effects of relative humidity, particle size and wall adhesion. *Powder Technol.* 2003;132:196–210.
62. Dart BL, Obendorf SK. Retention of *Aspergillus Niger* spores on textiles. In: Nelson CN, Henry NW, eds. *Performance of Protective Clothing: Issues and Priorities for the 21st*

Century. ASTM STP 1386. West Conshohocken, PA: American Society for Testing and Materials. 2000;7:251–268.

63. Li CS, Hou PA. Bioaerosol characteristics in hospital clean rooms. *Sci Total Environ.* 2003;305:169–176.
64. Kembel SW, Jones E, Kline J, et al. Architectural design influences the diversity and structure of the built environment microbiome. *ISME J.* 2012;6:1469–1479.
65. Claro T, O'Reilly M, Daniels S, Humphreys H. Surface microbial contamination in hospitals: A pilot study on methods of sampling and the use of proposed microbiologic standards. *Am J Infect Control.* 2015;43:1000–1002.
66. Russotto V, Cortegiani A, Raineri SM, Giarratano A. Bacterial contamination of inanimate surfaces and equipment in the intensive care unit. *J Intensive Care.* 2015;3:54.
67. Park H, Lee K, Kim M, Lee J, Seong SY, Ko G. Detection and hazard assessment of pathogenic microorganisms in medical wastes. *J Environ Sci Health A.* 2009;44:995–1003.
68. Pant D. Waste management in small hospitals: trouble for environment. *Environ Monit Assess.* 2012;184:4449–4453.
69. Wiener-Well Y, Galuty M, Rudensky B, Schlesinger Y, Attias D, Yinnon AM. Nursing and physician attire as possible source of nosocomial infections. *Am J Infect Control.* 2011;39:555–559.
70. Beggs C, Knibbs LD, Johnson GR, Morawska L. Environmental contamination and hospital-acquired infection: factors that are easily overlooked. *Indoor Air.* 2015;25:462–474.

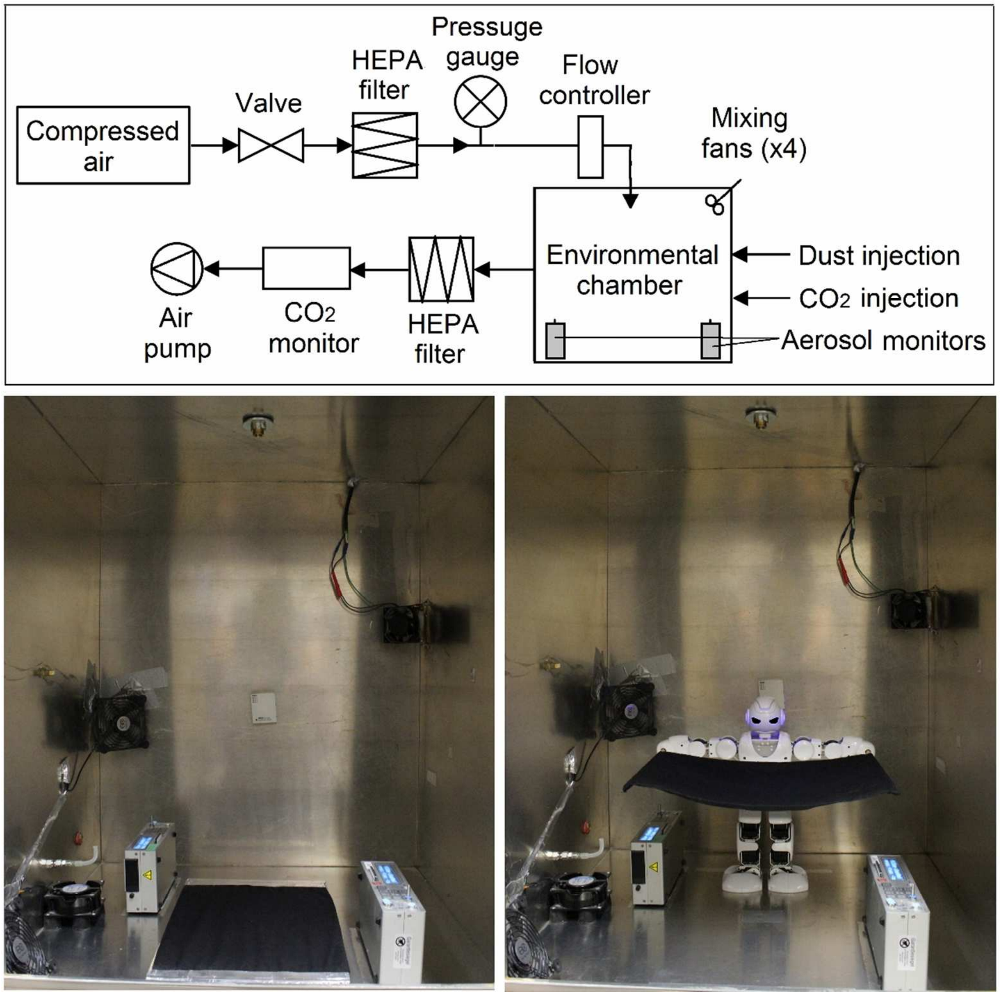

338x335mm (96 x 96 DPI)

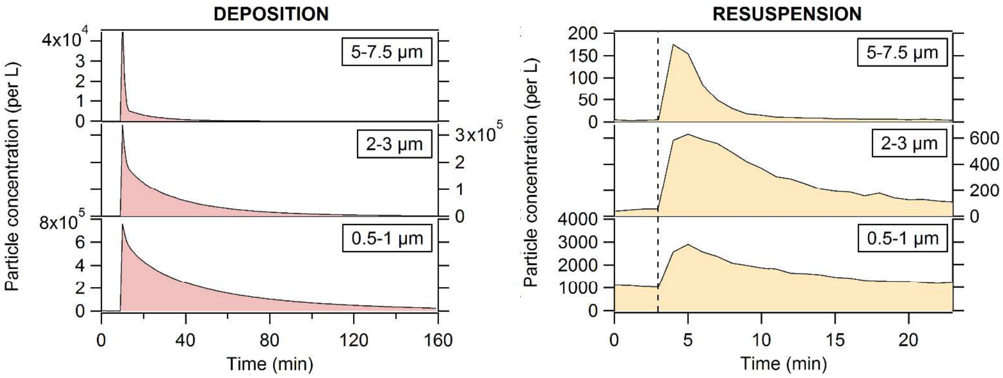
DEPOSITION
RESUSPENSION
5-7.5 µm
2-3 µm
0.5-1 µm
5-7.5 µm
2-3 µm
0.5-1 µm
Particle concentration (per L)
Particle concentration (per L)
4x10^4
3
2
1
0
3x10^5
2
1
0
8x10^5
6
4
2
0
0
40
80
120
160
Time (min)
200
150
100
50
0
600
400
200
0
4000
3000
2000
1000
0
0
5
10
15
20
Time (min)

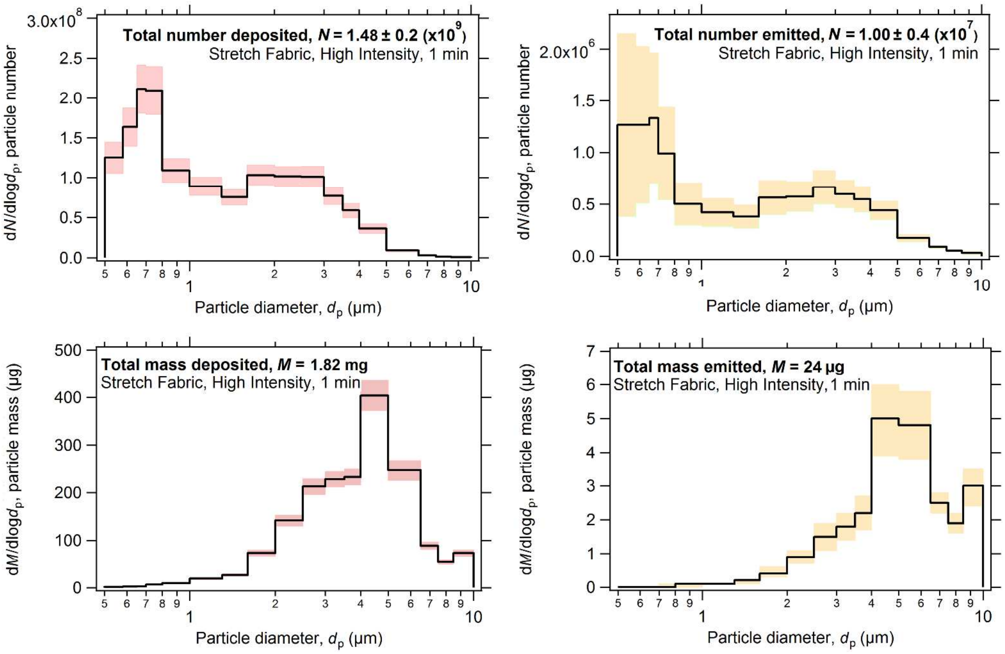
Total number deposited, *N* = 1.48 ± 0.2 (x10^9)
Stretch Fabric, High Intensity, 1 min
dN/dlogdp, particle number
3.0x10^8
2.5
2.0
1.5
1.0
0.5
0.0
5 6 7 8 9 1 2 3 4 5 6 7 8 9 10
Particle diameter, d_p (µm)
Total number emitted, *N* = 1.00 ± 0.4 (x10^7)
Stretch Fabric, High Intensity, 1 min
dN/dlogdp, particle number
2.0x10^6
1.5
1.0
0.5
0.0
Particle diameter, d_p (µm)
Total mass deposited, *M* = 1.82 mg
Stretch Fabric, High Intensity, 1 min
dM/dlogdp, particle mass (µg)
500
400
300
200
100
0
Particle diameter, d_p (µm)
Total mass emitted, *M* = 24 µg
Stretch Fabric, High Intensity,1 min
dM/dlogdp, particle mass (µg)
7
6
5
4
3
2
1
0
Particle diameter, d_p (µm)

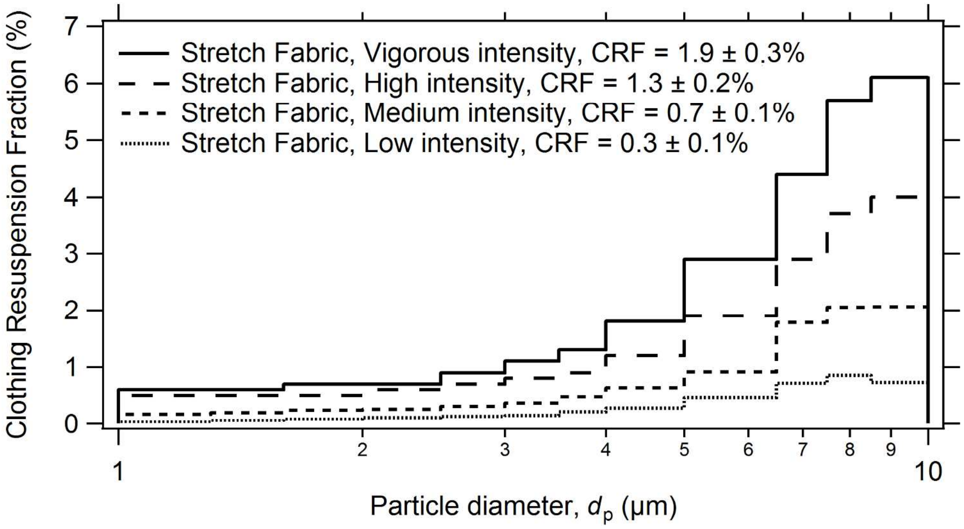
Stretch Fabric, Vigorous intensity, CRF = 1.9 ± 0.3%
Stretch Fabric, High intensity, CRF = 1.3 ± 0.2%
Stretch Fabric, Medium intensity, CRF = 0.7 ± 0.1%
Stretch Fabric, Low intensity, CRF = 0.3 ± 0.1%
Clothing Resuspension Fraction (%)
0
1
2
3
4
5
6
7
1
2
3
4
5
6
7
8
9
10
Particle diameter, d_p (µm)

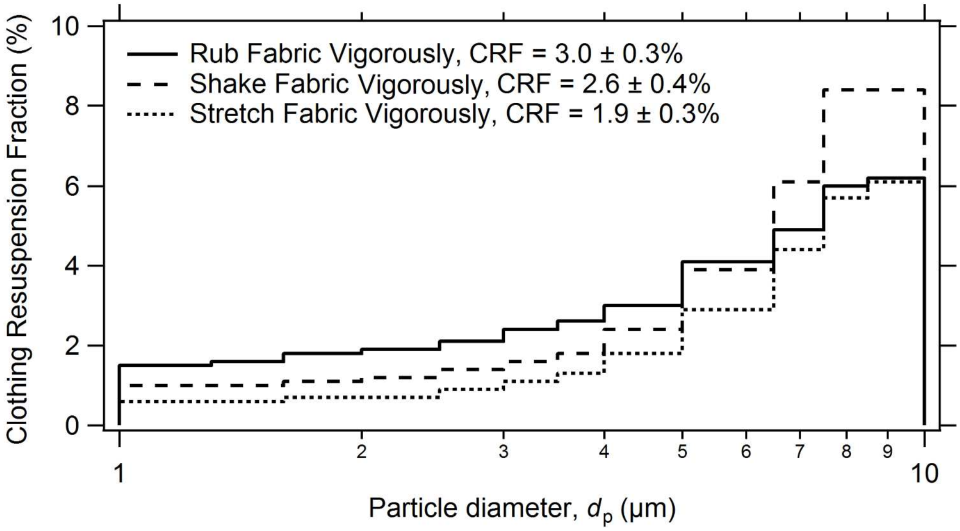
Rub Fabric Vigorously, CRF = 3.0 ± 0.3%
Shake Fabric Vigorously, CRF = 2.6 ± 0.4%
Stretch Fabric Vigorously, CRF = 1.9 ± 0.3%
Clothing Resuspension Fraction (%)
0
2
4
6
8
10
1
2
3
4
5
6
7
8
9
10
Particle diameter, d_p (μm)

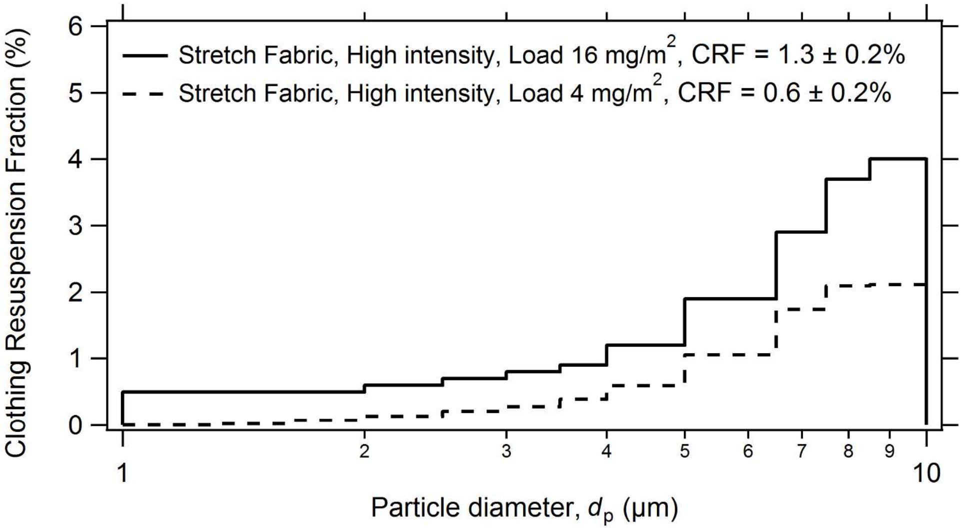
Stretch Fabric, High intensity, Load 16 mg/m2, CRF = 1.3 ± 0.2%
Stretch Fabric, High intensity, Load 4 mg/m2, CRF = 0.6 ± 0.2%
Clothing Resuspension Fraction (%)
0
1
2
3
4
5
6
1
2
3
4
5
6
7
8
9
10
Particle diameter, dp (μm)

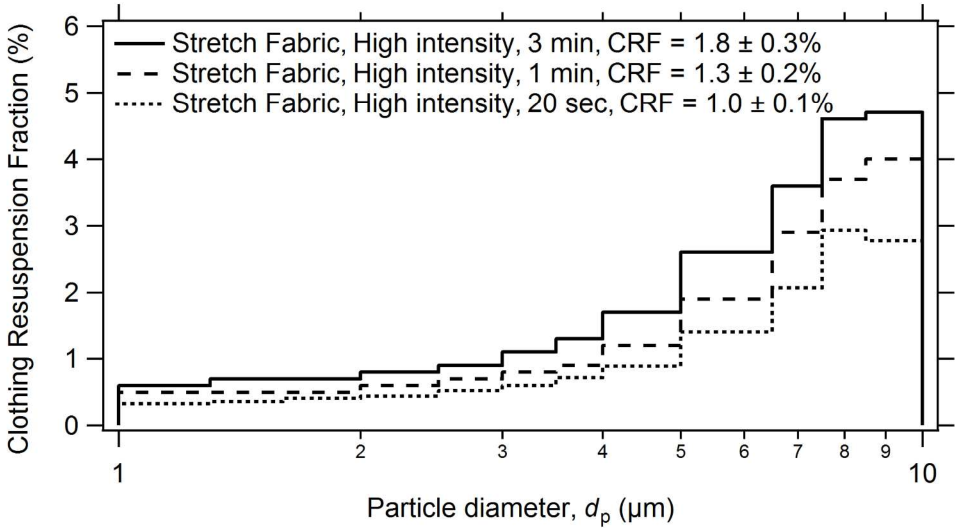
Stretch Fabric, High intensity, 3 min, CRF = 1.8 ± 0.3%
Stretch Fabric, High intensity, 1 min, CRF = 1.3 ± 0.2%
Stretch Fabric, High intensity, 20 sec, CRF = 1.0 ± 0.1%
Clothing Resuspension Fraction (%)
0
1
2
3
4
5
6
1
2
3
4
5
6
7
8
9
10
Particle diameter, d_p (μm)

Online Supporting Information

Clothing as a transport vector for airborne particles: Chamber study

Dusan Licina*, William W Nazaroff

Department of Civil and Environmental Engineering, University of California, Berkeley, California 94720, United States of America

*Corresponding email: licinadusan@yahoo.com

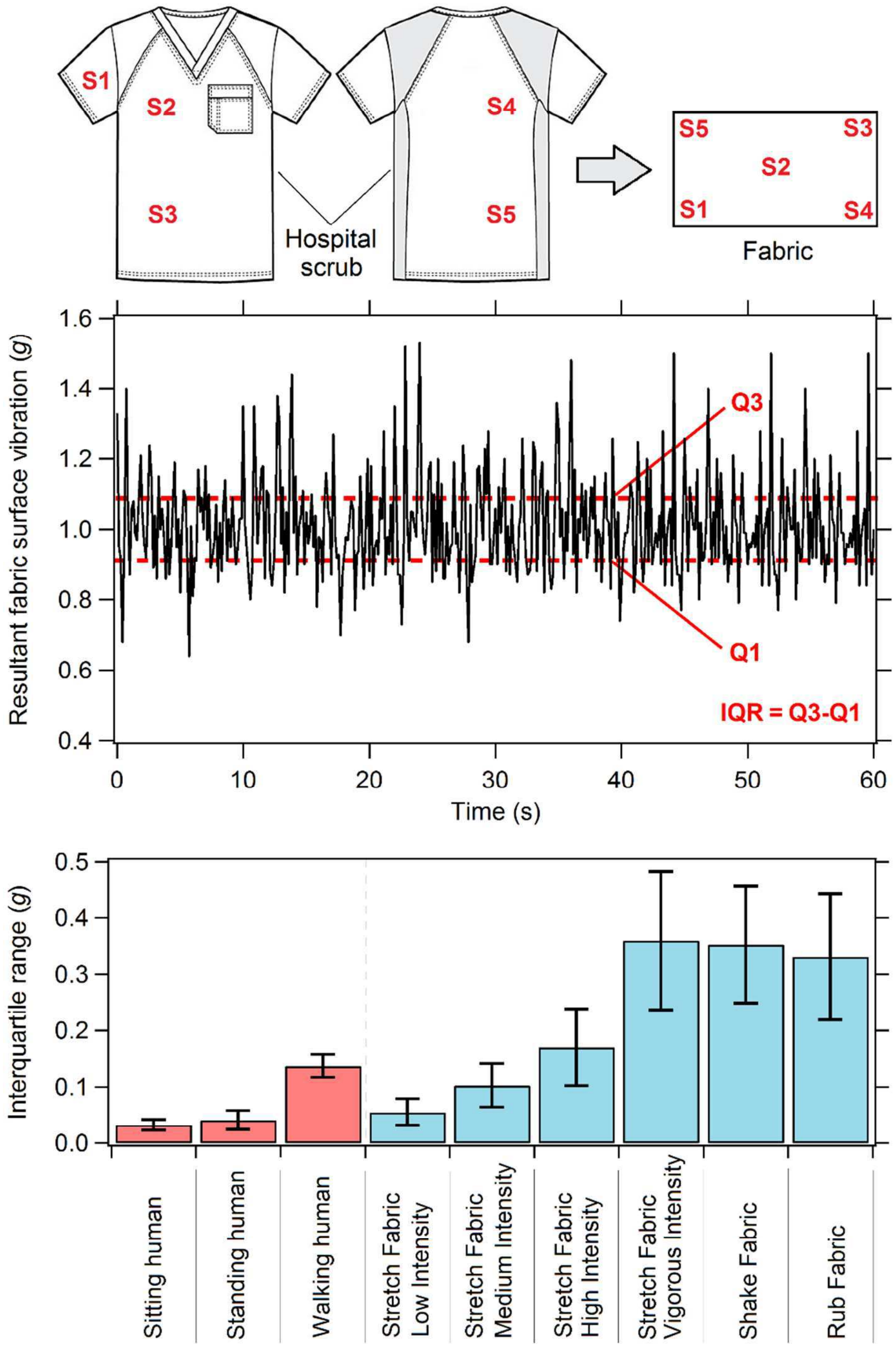

Fig. S1 (Upper frame) Placement of five automated vibrational accelerometers on a hospital scrub (data collected from both left and right side of the scrub; 10 locations in total) and the fabric; (middle frame) example of the real-time resultant clothing surface vibrations during a fabric manipulation experiment (ID=3); (lower frame) the interquartile range of the hospital scrub resultant surface vibrations for real human experiments and the interquartile range of the fabric resultant surface vibrations across controlled resuspension experiments performed with the robot. Note that standard deviation corresponds to different sensor placement on a hospital scrub/fabric. Standard deviation for repeated runs was very small (≤ 0.01 *g*).

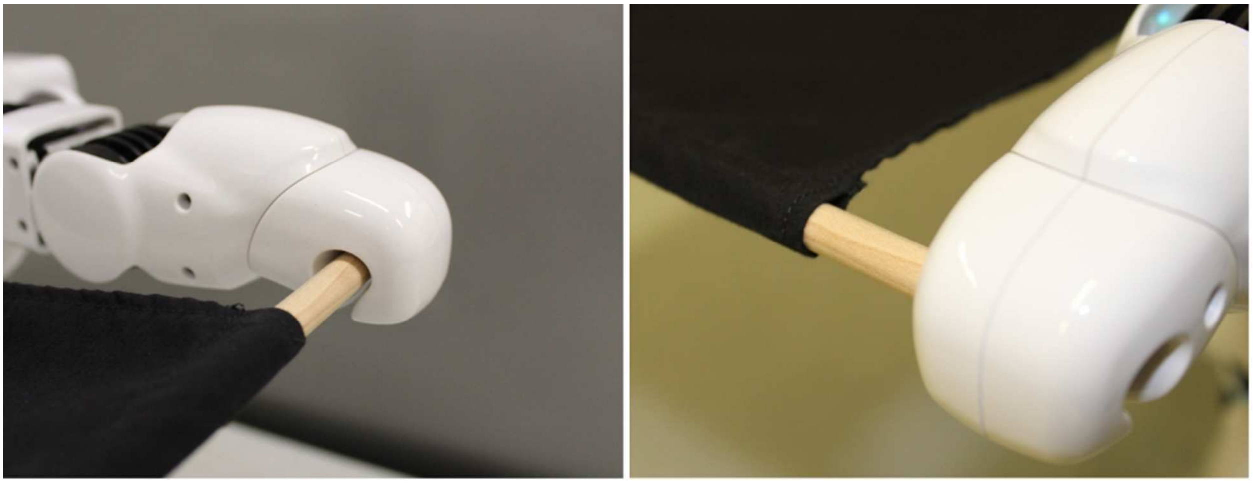

Fig. S2 Illustration of fabric attachment to custom-made wooden fabric holders fixed to the robot.

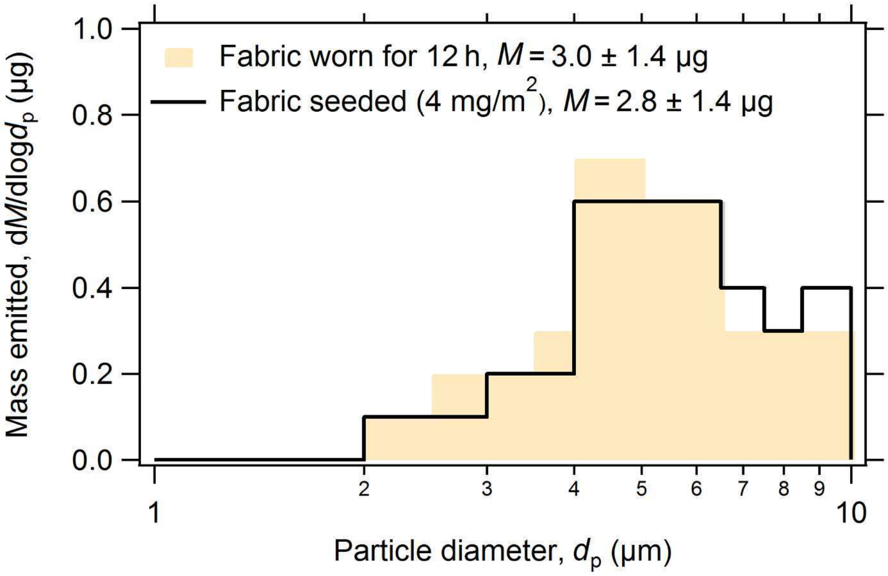

Fig. S3 Comparison between size-resolved particle mass concentration (mean ± standard deviation, $n = 3$) emitted as a consequence of stretching fabric with high intensity, when the fabric was attached to the subject's chest and worn for 12 h, and when the fabric was contaminated with a particle loading of 4 mg/m^2.

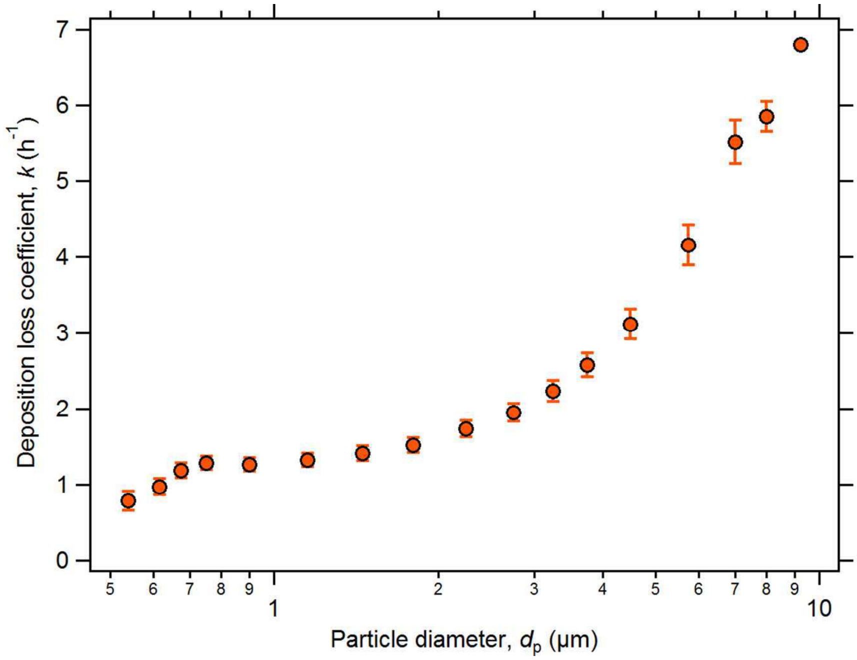

d_p size bin (μm)	k (h^{-1}) (n = 30)
0.50 - 0.58	0.79 ± 0.12
0.58 - 0.65	0.97 ± 0.11
0.65 - 0.70	1.19 ± 0.10
0.70 - 0.80	1.28 ± 0.09
0.80 - 1.00	1.26 ± 0.09
1.00 - 1.30	1.33 ± 0.09
1.30 - 1.60	1.41 ± 0.09
1.60 - 2.00	1.52 ± 0.10
2.00 - 2.50	1.74 ± 0.10
2.50 - 3.00	1.95 ± 0.12
3.00 - 3.50	2.23 ± 0.14
3.50 - 4.00	2.58 ± 0.16
4.00 - 5.00	3.12 ± 0.19
5.00 - 6.50	4.15 ± 0.26
6.50 - 7.50	5.52 ± 0.28
7.50 - 8.50	5.85 ± 0.19
8.50 - 10.0	6.80 ± 0.01

Fig. S4 Graphical and tabular representation of empirically derived size-resolved deposition loss rate coefficients (mean ± standard deviation, n = 30).

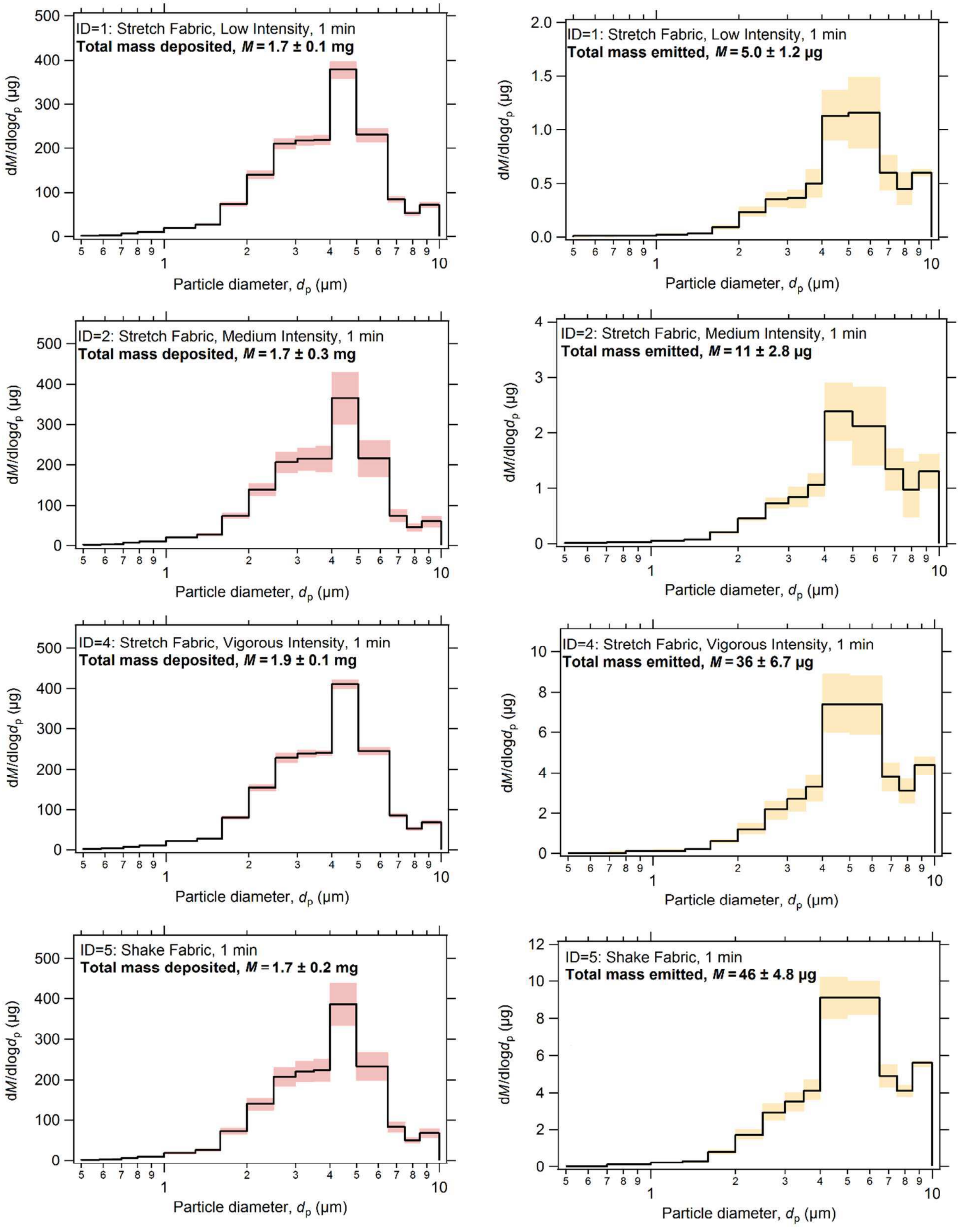
ID=1: Stretch Fabric, Low Intensity, 1 min
Total mass deposited, M = 1.7 ± 0.1 mg
ID=1: Stretch Fabric, Low Intensity, 1 min
Total mass emitted, M = 5.0 ± 1.2 µg
ID=2: Stretch Fabric, Medium Intensity, 1 min
Total mass deposited, M = 1.7 ± 0.3 mg
ID=2: Stretch Fabric, Medium Intensity, 1 min
Total mass emitted, M = 11 ± 2.8 µg
ID=4: Stretch Fabric, Vigorous Intensity, 1 min
Total mass deposited, M = 1.9 ± 0.1 mg
ID=4: Stretch Fabric, Vigorous Intensity, 1 min
Total mass emitted, M = 36 ± 6.7 µg
ID=5: Shake Fabric, 1 min
Total mass deposited, M = 1.7 ± 0.2 mg
ID=5: Shake Fabric, 1 min
Total mass emitted, M = 46 ± 4.8 µg
dM/dlogdp (µg)
Particle diameter, dp (µm)
0
100
200
300
400
500
0.0
0.5
1.0
1.5
2.0
1
2
3
4
6
8
10
12
5
6
7
8
9
1
2
3
4
5
6
7
8
9
10

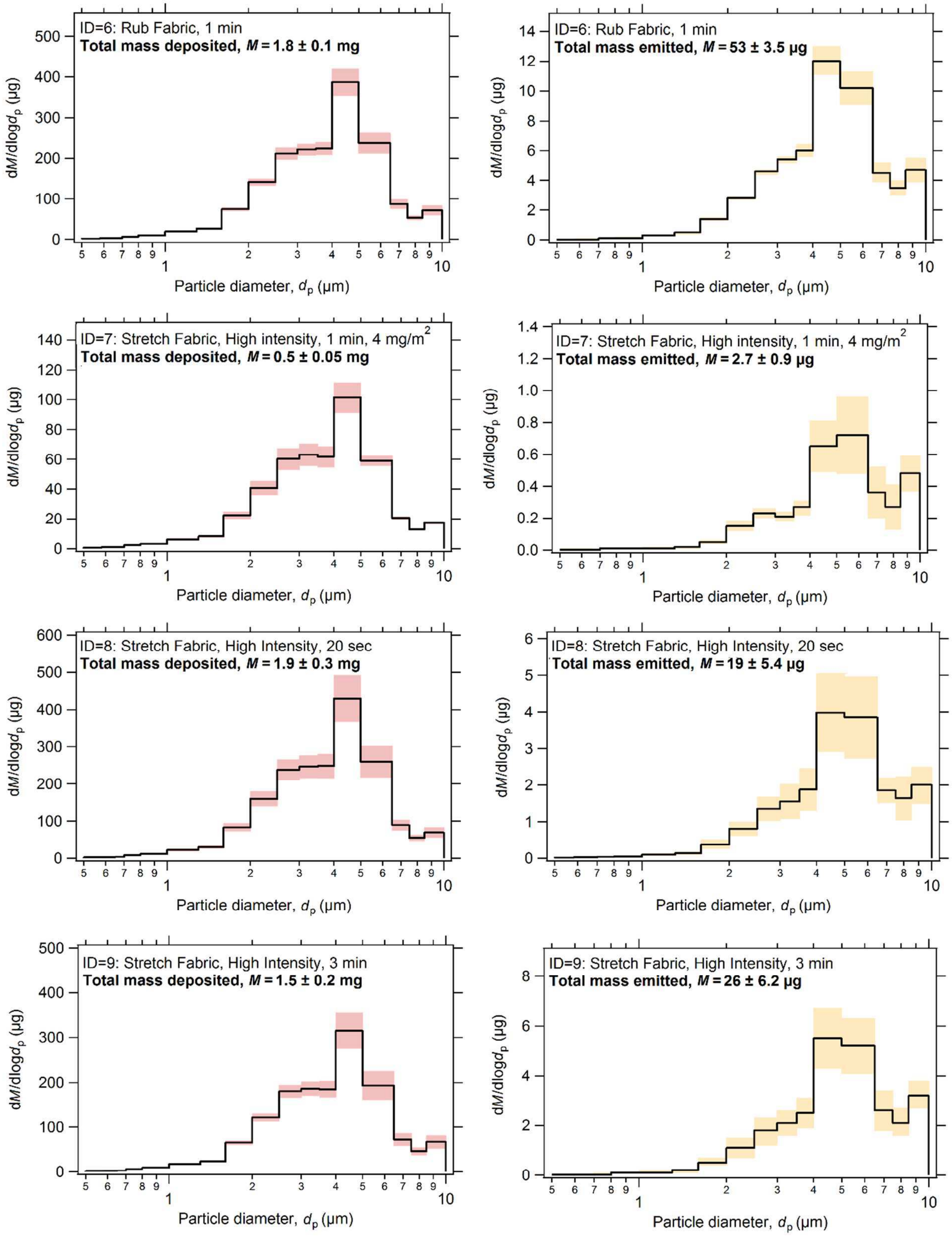

Fig. S5 Average mass-weighted size distribution during deposition event (left frames) and resuspension event as a consequence of manipulating fabric (right frames). The mean ± standard deviation (illustrated by shaded area) across specified particle sizes are reported in each frame.

Table S1 Detailed description of the volunteer activity type and duration.

ID	Volunteer activity	Time intervals (sec)	Description
1	Sitting while handling an infant	0-2; 16-18; 31-33; 46-48	Picking up an infant (simulated, no infant)
		3-12; 19-27; 34-42; 49-57	Handling and lightly swinging an infant (simulated, no infant)
		13-15; 28-30; 43-45; 58-60	Put down an infant (simulated, no infant)
2	Standing while handling an infant	0-2; 16-18; 31-33; 46-48	Picking up an infant (simulated, no infant)
		3-12; 19-27; 34-42; 49-57	Handling and lightly swinging an infant (simulated, no infant)
		13-15; 28-30; 43-45; 58-60	Put down an infant (simulated, no infant)
3	Walking at a constant pace (100 steps/min)	0-60	Walking at a constant speed of 1.3 m/s.

Video material:

Video S1. Stretch Fabric, Low Intensity (ID = 1) https://youtu.be/wTQ_tSpgwrs

Video S2. Stretch Fabric, Medium Intensity (ID = 2) https://youtu.be/ybeufdmF1AY

Video S3. Stretch Fabric, High Intensity (ID = 3) https://youtu.be/vE3Djzmmm8Q

Video S4. Stretch Fabric, Vigorous Intensity (ID = 4) https://youtu.be/YfOjAorua3k

Video S5. Shake Fabric, Vigorous Intensity (ID = 5) https://youtu.be/GR3GkrbrqiM

Video S6. Rub Fabric, Vigorous Intensity (ID = 6) https://youtu.be/QuK6bLQO3Jk

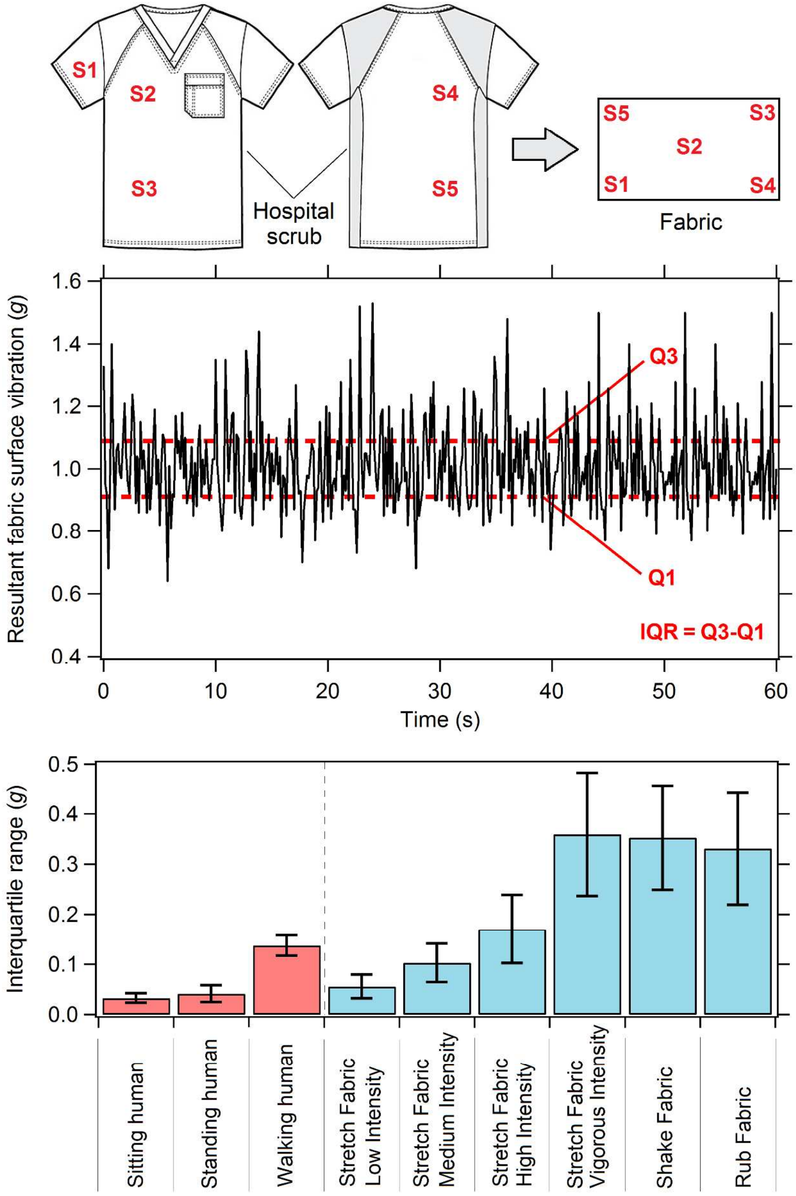
S1
S2
S3
S4
S5
Hospital scrub
S5
S3
S2
S1
S4
Fabric
Resultant fabric surface vibration (g)
1.6
1.4
1.2
1.0
0.8
0.6
0.4
Q3
Q1
IQR = Q3-Q1
0
10
20
30
40
50
60
Time (s)
Interquartile range (g)
0.5
0.4
0.3
0.2
0.1
0.0
Sitting human
Standing human
Walking human
Stretch Fabric Low Intensity
Stretch Fabric Medium Intensity
Stretch Fabric High Intensity
Stretch Fabric Vigorous Intensity
Shake Fabric
Rub Fabric

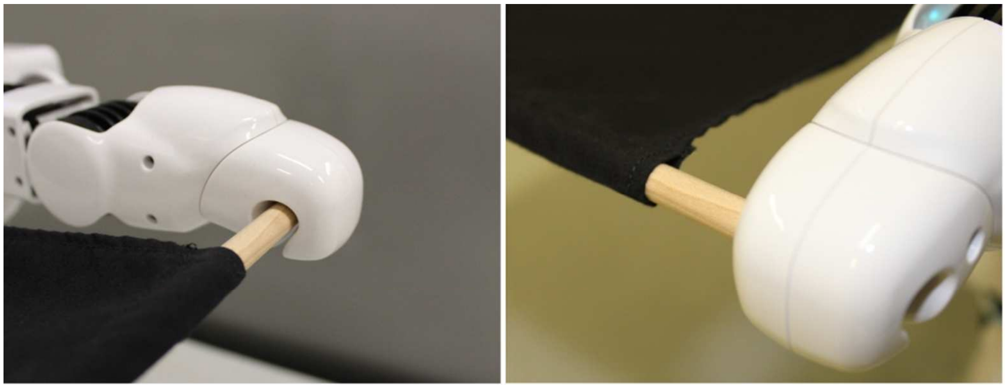

361x137mm (72 x 72 DPI)

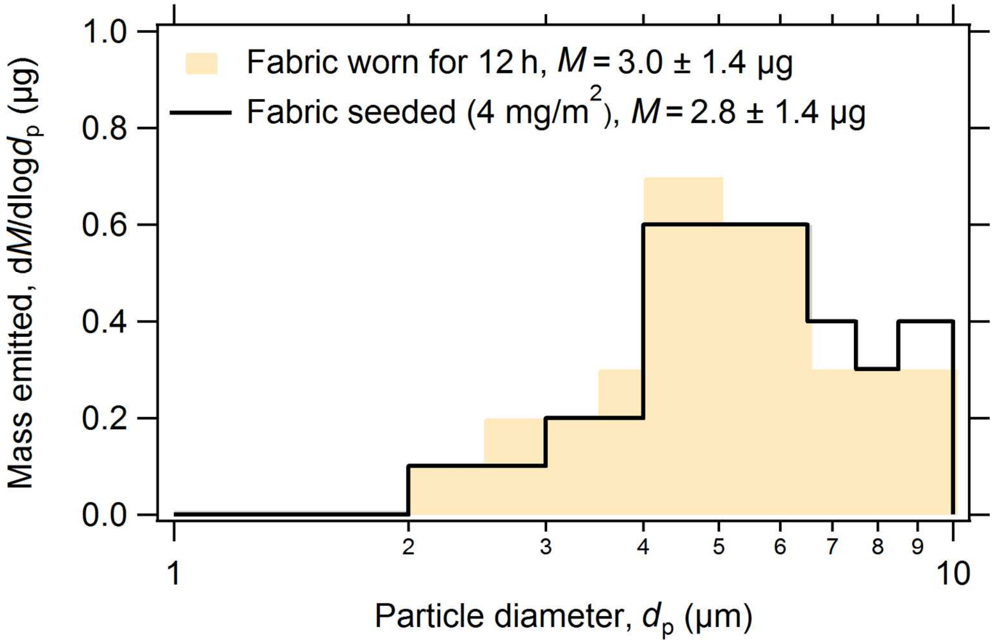
Fabric worn for 12 h, $M = 3.0 \pm 1.4$ µg
Fabric seeded (4 mg/m^2), $M = 2.8 \pm 1.4$ µg
Mass emitted, dM/dlogd_p (µg)
1.0
0.8
0.6
0.4
0.2
0.0
1
2
3
4
5
6
7
8
9
10
Particle diameter, d_p (µm)

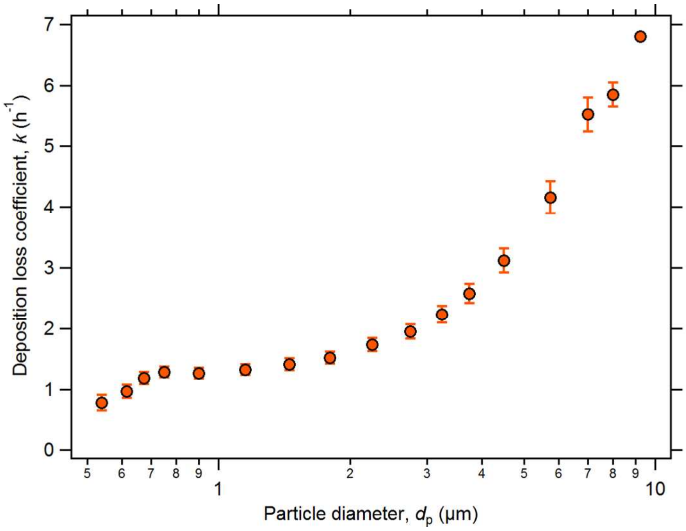

d_p size bin (μm)	k (h^{-1}) (n = 30)
0.50 - 0.58	0.79 ± 0.12
0.58 - 0.65	0.97 ± 0.11
0.65 - 0.70	1.19 ± 0.10
0.70 - 0.80	1.28 ± 0.09
0.80 - 1.00	1.26 ± 0.09
1.00 - 1.30	1.33 ± 0.09
1.30 - 1.60	1.41 ± 0.09
1.60 - 2.00	1.52 ± 0.10
2.00 - 2.50	1.74 ± 0.10
2.50 - 3.00	1.95 ± 0.12
3.00 - 3.50	2.23 ± 0.14
3.50 - 4.00	2.58 ± 0.16
4.00 - 5.00	3.12 ± 0.19
5.00 - 6.50	4.15 ± 0.26
6.50 - 7.50	5.52 ± 0.28
7.50 - 8.50	5.85 ± 0.19
8.50 - 10.0	6.80 ± 0.01

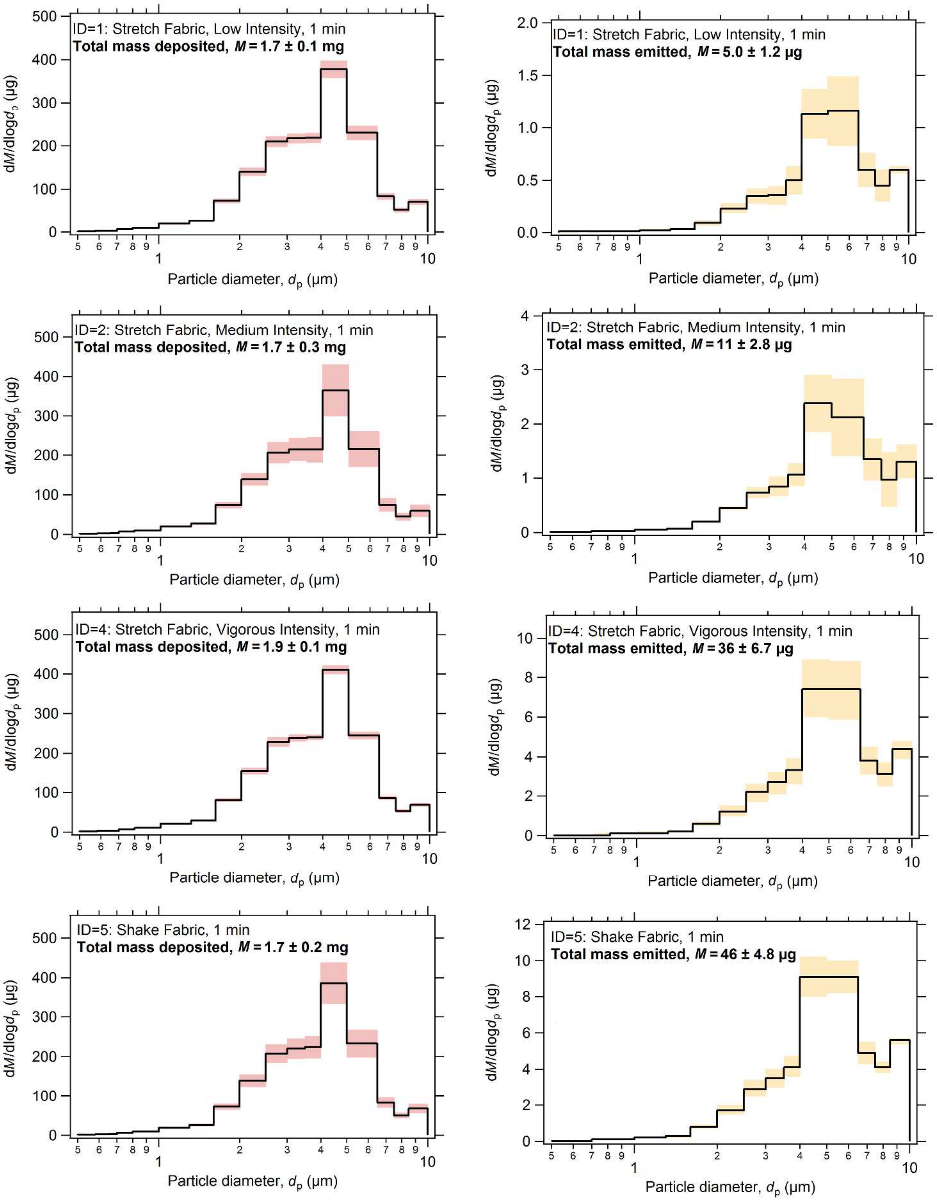
ID=1: Stretch Fabric, Low Intensity, 1 min
Total mass deposited, M = 1.7 ± 0.1 mg
ID=1: Stretch Fabric, Low Intensity, 1 min
Total mass emitted, M = 5.0 ± 1.2 µg
ID=2: Stretch Fabric, Medium Intensity, 1 min
Total mass deposited, M = 1.7 ± 0.3 mg
ID=2: Stretch Fabric, Medium Intensity, 1 min
Total mass emitted, M = 11 ± 2.8 µg
ID=4: Stretch Fabric, Vigorous Intensity, 1 min
Total mass deposited, M = 1.9 ± 0.1 mg
ID=4: Stretch Fabric, Vigorous Intensity, 1 min
Total mass emitted, M = 36 ± 6.7 µg
ID=5: Shake Fabric, 1 min
Total mass deposited, M = 1.7 ± 0.2 mg
ID=5: Shake Fabric, 1 min
Total mass emitted, M = 46 ± 4.8 µg
dM/dlogdp (µg)
Particle diameter, dp (µm)
0
100
200
300
400
500
0.0
0.5
1.0
1.5
2.0
1
2
3
4
6
8
10
12
5 6 7 8 9 1 2 3 4 5 6 7 8 9 10

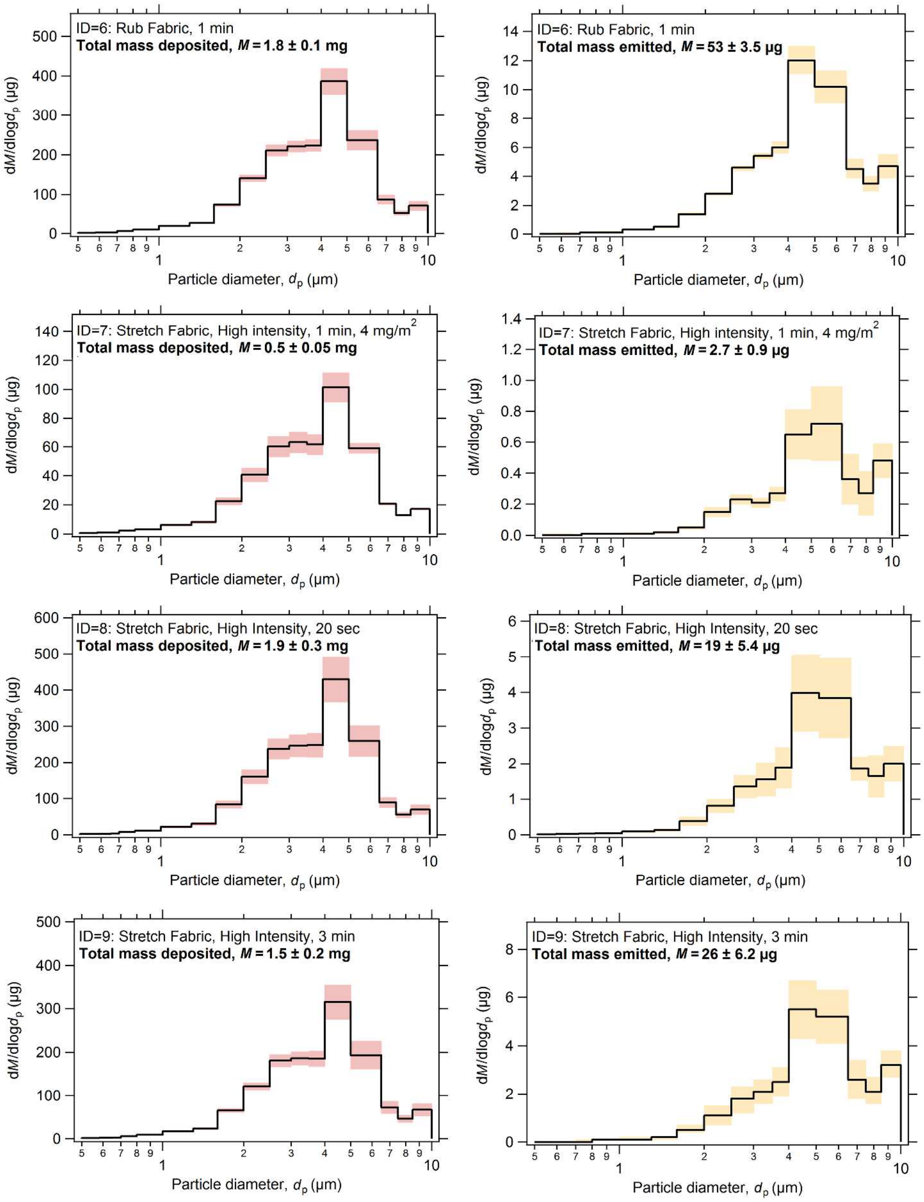
ID=6: Rub Fabric, 1 min
Total mass deposited, M = 1.8 ± 0.1 mg
ID=6: Rub Fabric, 1 min
Total mass emitted, M = 53 ± 3.5 µg
ID=7: Stretch Fabric, High intensity, 1 min, 4 mg/m2
Total mass deposited, M = 0.5 ± 0.05 mg
ID=7: Stretch Fabric, High intensity, 1 min, 4 mg/m2
Total mass emitted, M = 2.7 ± 0.9 µg
ID=8: Stretch Fabric, High Intensity, 20 sec
Total mass deposited, M = 1.9 ± 0.3 mg
ID=8: Stretch Fabric, High Intensity, 20 sec
Total mass emitted, M = 19 ± 5.4 µg
ID=9: Stretch Fabric, High Intensity, 3 min
Total mass deposited, M = 1.5 ± 0.2 mg
ID=9: Stretch Fabric, High Intensity, 3 min
Total mass emitted, M = 26 ± 6.2 µg
dM/dlogdp (µg)
Particle diameter, dp (µm)
1
10